Journal of Nuclear Materials 587 (2023) 154744

Contents lists available at ScienceDirect

Journal of Nuclear Materials

journal homepage: www.elsevier.com/locate/jnucmat

The SCIANTIX code for fission gas behaviour: Status, upgrades, separate-effect validation, and future developments

G. Zullo, D. Pizzocri, L. Luzzi *

Department of Energy, Nuclear Engineering Division, Politecnico di Milano, Via La Masa 34, Milan 20156, Italy

HIGHLIGHTS

- The new version of the SCIANTIX code is described.
- The new SCIANTIX modelling capabilities are detailed.
- The code structure and its numerical features are presented.
- Each model is presented with the separate-effect validation database.
- Future model developments and qualification actions are outlined.

ARTICLE INFO

Keywords:
SCIANTIX
Physics-based modelling
Fission gas behaviour
Nuclear fuel

ABSTRACT

SCIANTIX is a 0D, open-source code designed to model inert gas behaviour within nuclear fuel at the scale of the grain. The code predominantly employs mechanistic approaches based on kinetic rate-theory models to calculate engineering quantities, such as fission gas release and gaseous fuel swelling. Since its release, SCIANTIX has undergone significant improvements, including the incorporation of new modelling and numerical capabilities. The code architecture has been revamped, embracing an object-orientated structure improving the overall efficiency and usability. This work provides a concise overview of the current state of the SCIANTIX code, highlighting recent updates and advancements. Each SCIANTIX model is presented along with the corresponding separate-effect validation database, which is used to assess its accuracy and predictions.

1. Introduction

Understanding and predicting the behaviour of inert gases in nuclear fuel is vital to ensure reliable and efficient operation of fuel rods, and the safety of light water and fast reactors [1–5]. Physics-based approaches based on kinetic rate-theory models [6–11], and corresponding codes [12–24], have been developed to capture the intricate inert gas behaviour (IGB) in nuclear fuel. The use of kinetic rate-theory models is motivated by several inherent advantages. First of all, description with a limited set of differential equations governing different phenomena [25–28]; the natural application of the simulation to a wide range of operational and accidental transient scenarios [7,9,12,29–32]; the direct benefit from new separate-effect experimental data available, hence extending the separate-effect validation database of the implemented models [28,33,34]. Lastly, by bridging information from lower-length scales (e.g., by definition of specific model parameters [12, 35–42]) to engineering scale of the nuclear fuel rod, easing the applicability to different fuel materials (e.g., by modifying specific material properties) with minor modifications. Among the developed mesoscopic codes dealing with physics-based IGB modelling, none are open source [12,20,43], hindering their applicability in the frame of multi-scale and multi-physical projects involving different software. Therefore, SCIANTIX was developed with the goal of being an open-source, standalone code for IGB physics-based modelling, applicable to simulations of experiments with separate effects on the fuel-grain scale, or generally for samples in uniform conditions, supporting both the design of the experiment itself and the interpretation of the results [22].

On the engineering scale, fuel performance codes (FPCs) are fundamental to predict the behaviour of fuel rods, encompassing different operating conditions such as normal operation, accidents, and dry storage [3,44–50]. Notably, FPCs are currently being developed to enable multi-dimensional simulations (1D, 1.5D, 2D, 3D) and

* Corresponding author.
E-mail address: lelio.luzzi@polimi.it (L. Luzzi).

https://doi.org/10.1016/j.jnucmat.2023.154744
Received 20 July 2023; Received in revised form 15 September 2023; Accepted 18 September 2023
Available online 19 September 2023

physics-based modelling by coupling with dedicated meso-scale modules [50–52]. The coupling of FPCs with the SCIANTIX code has proven to be beneficial for the integral fuel rod simulation [51,53–57], since SCIANTIX is able to effectively bridge lower-length scale information (e.g., by informing/updating parameters from experiments, or molecular dynamics/phase field simulation [58,59]) to the rod engineering scale, acting as physics-based IGB module (online coupling) within the FPC, with an emphasis on maintaining a limited CPU time on the overall integral simulation [53,55,60]. For this reason, separate ongoing work by the authors will focus on the validation of the SCIANTIX code, coupled with FPCs, against integral irradiation experiments.

SCIANTIX is currently available as an open-source code under MIT license, greatly easing its usage as IGB module in existing FPCs. Because of this licensing choice, all the implemented models are already published and validated against separate-effect experiments. The choice of such license is a fundamental point for the application of SCIANTIX as IGB module: typically, FPCs are not available as open-source software,[1] and sharing development within the context of collaborative international projects and educational initiatives, including mobility programs for students and young researchers, can pose challenges. The integration of open-source tools like SCIANTIX within the FPC infrastructure offers a promising solution to this limitation. Given the open-source nature of SCIANTIX, standardised qualification and quality assurance guidelines are being considered and directly integrated in the source code and in its online repository [61–65]. The code repository is available online at [66,67], including the validation database of the implemented SCIANTIX models, and non-regression testing tools and continuous integration services. These services are going to be further extended and developed, to improve the process of testing new code versions and branches, and to clarify guidelines for contributors.

This work is organized as follows. Section 2 explains the structure of the code and its numerical features. Section 3 collects the physics-based models available in SCIANTIX. Section 4 illustrates the results of SCIANTIX calculations against experimental data. Section 5 discusses simulation results, including important model parameters and current code limitations, and future developments as well. Finally, Section 6 draws conclusions of the work.

Nomenclature [a]

A_{gf}	Inter-granular bubble projected area	m^2 bub^{-1}
a	Spherical grain radius	m
b	Intra-granular irradiation-induced resolution rate	s^{-1}
c	Single-atom gas concentration	at m^{-3}
c_{lim}	Solubility	at m^{-3}
D	Intra-granular diffusivity	m^2 s^{-1}
D_{gr}	Average grain size	m
f	Intactness of grain faces	/
F	Fission rate density	fiss m^{-3} s^{-1}
F_{gf}	Fractional coverage of grain faces	/
$F_{gf,\ sat}$	Saturation fractional coverage of grain faces	/
g	Intra-granular trapping rate	s^{-1}
k_H	Henry's constant	at m^{-3} MPa^{-1}
k^*	Grain growth rate constant	m^2 s^{-1}
m	Gas concentration in intra-granular bubbles	at m^{-3}
N_{ig}	Intra-granular bubble concentration	bub m^{-3}
N_{gf}	Inter-granular bubble concentration	bub m^{-2}
p	Pressure	MPa
q	Inter-granular gas concentration	at m^{-3}
R	Release rate	at m^{-3} s^{-1}
R_{ig}	Intra-granular bubble radius	m bub^{-1}
R_{ff}	Fission fragment influence radius	m
R_{gf}	Inter-granular bubble radius	m bub^{-1}
r	Radial coordinate	m
S	Intra-granular gas production rate	at m^{-3} s^{-1}
T	Temperature	K
t	Time	s
y	Cumulative fission yield	at $fiss^{-1}$
Z	Compressibility factor	/
α	Precursor enhancement factor	/
β	Burnup	MWd kgU^{-1}
γ	Intra-granular thermal re-solution rate	s^{-1}
$(\Delta V/V)_{ig}$	Intra-granular swelling	/
$(\Delta V/V)_{gf}$	Inter-granular swelling	/
k_B	Boltzmann constant	J K^{-1}
λ	Decay rate	s^{-1}
μ_{ff}	Fission fragment range	m
ν	Intra-granular nucleation rate	bub m^{-3} s^{-1}
σ_h	Hydrostatic fuel stress	MPa

[a]: at stands for atoms, fiss for fissions, bub for bubbles.

2. Code structure and numerical features

The current release of SCIANTIX (version 2.0) marks a significant advancement with respect to the first release of the code [22]. The code architecture has been revamped, embracing an object-orientated structure that improves overall efficiency and usability, providing a streamlined and organised structure. An intuitive and modular inclusion of several quantities relevant to the SCIANTIX simulation has been realised, representing fuel matrix properties (e.g., UO_2 lattice parameter), specific gas atoms (xenon, krypton, helium), IGB models, and numerical solvers. This modular design enhances flexibility and extensibility of the code, enabling the expansion of its capabilities, e.g., by incorporating new material properties via available experimental data or atomistic/molecular dynamics simulation. Fig. 1 illustrates the flow chart of the SCIANTIX code. On the left side, basic features of SCIANTIX are represented. At the beginning of the simulation, SCIANTIX elaborates the input quantities provided by the user. Fuel matrix (e.g., UO_2), gas atoms (e.g., xenon and krypton) and corresponding systems of gas atoms inside the fuel matrix are prepared. Afterwards, each IGB model is constructed, including model parameters. In an independent way, numerical solvers required by the models are declared. The separation of the SCIANTIX models from the numerical solvers allows carrying out independent verification and separate-effect validation phases.

The right side of Fig. 1 shows the SCIANTIX external driver, the latter being the external user in the code standalone version or the FPC if SCIANTIX is used as IGB coupled module. SCIANTIX retains the same interface to preserve the coupling currently in place with FPCs (e.g., TRANSURANUS [53,56] and GERMINAL [68], OFFBEAT [49,52,69] and FRAPCON/FRAPTRAN [49,69]). A separate work of the authors (under preparation) will deepen the aspects related to the SCIANTIX coupling with FPCs.

Since SCIANTIX is also designed to be coupled with FPCs, the computational time taken by the simulation is an important aspect. Each SCIANTIX model includes a set of ODEs/PDEs, as it is described in the next sections. In order to reduce the computational time taken by the simulation, the solution of the set of the fully-coupled differential equations is approximated by using a segregated solution scheme[2] (or operator split approach) [70]. The differential equations considered in SCIANTIX are solved with an implicit L-stable scheme of the first order, i.e., backward Euler. As a results, all numerical solutions are consistent. The numerical solvers belong to an independent class, which depends only on the user input (e.g., in the choice of the specific solver, as shown

[1] Some exceptions are worth mentioning, e.g., the OFFBEAT code [52], already coupled to SCIANTIX, and in general the ONCORE/IAEA involved codes [81,138].

[2] The operator-splitting scheme simplifies the treatment of non-linearities in state variables and model parameters and complies with the computational time typical of a meso-scale module. Even if the operator-splitting represents a numerical approximation, experience with SCIANTIX has shown that it is suitable for fission gas behaviour modelling in constant and transient conditions.

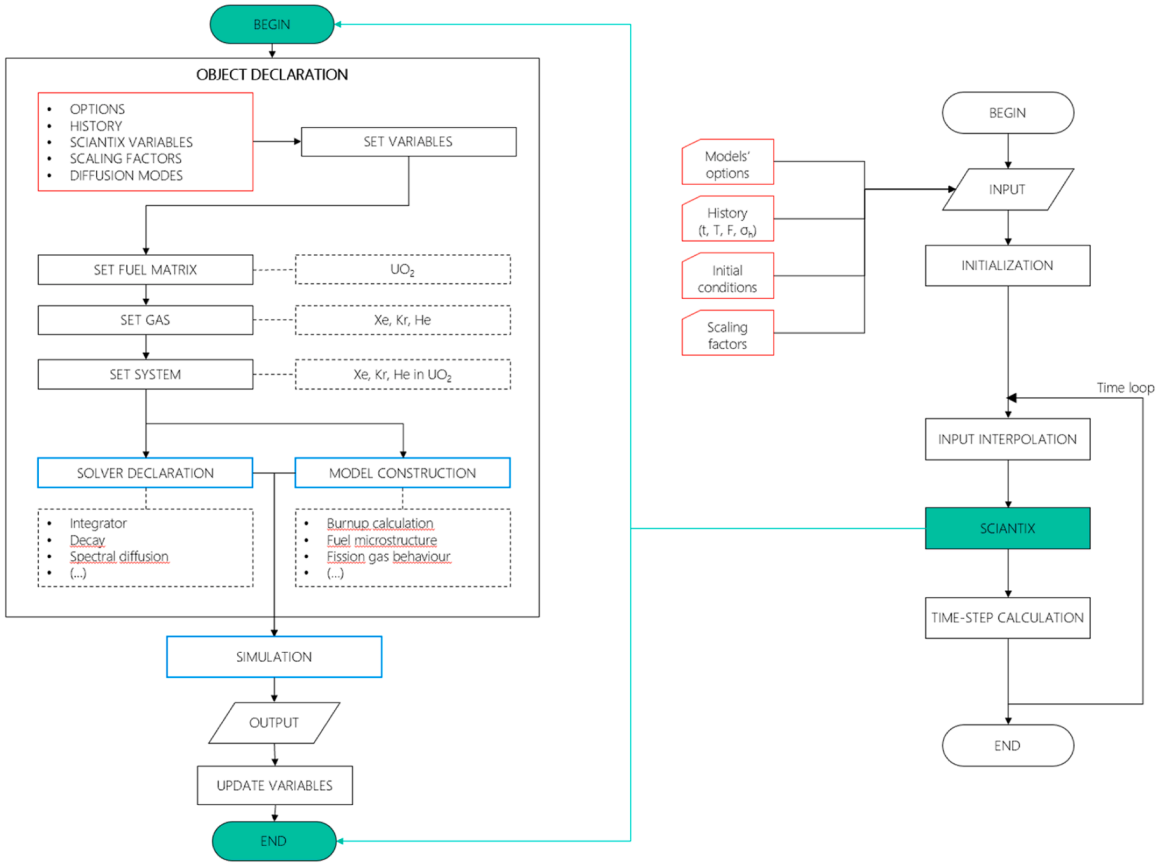

Fig. 1. Flowchart of SCIANTIX 2.0. The external driver (parent code, on the right) preserves the coupling currently in place with fuel performance codes. The meso-scale module (on the left) schematically shows how the construction of specific objects for inert gas behaviour modelling is developed. It is also emphasized the logic by which the SCIANTIX simulation is obtained after the communication of specific solvers with the constructed models.

in Fig. 2 where the objects hierarchical approach is illustrated) and can be recalled in the different models. Furthermore, comprehensive verification processes have been realized for each solver through the method of manufactured solution (MMS) [71,72], and made available on the code repository [66,67]. This organic verification approach allows developers of physical models to prioritize their attention on the underlying physical phenomena, disregarding errors of numerical nature.

Concerning the coupling of SCIANTIX with FPCs working as an IGB module, the coupling has been positively carried out and demonstrated with TRANSURANUS [74] and GERMINAL [75] in the frame of the INSPYRE Project [76], with applications to fast reactor conditions. Currently, SCIANTIX coupled with TRANSURANUS is extensively adopted in the PATRICIA project [77], with application to americium-bearing nuclear fuels [78], and developments towards the helium production rate modelling [79]. In the frame of the R2CA project [80], SCIANTIX has been successfully coupled with FRAPCON [69] and FRAPTRAN [49], where it has been applied to LWR nominal and accidental conditions. The open-source code OFFBEAT employs SCIANTIX as standard fission gas behaviour module [51,52], playing a key role in the OperaHPC project [81]. Description and discussion of the integral validation (i.e., against integral irradiation experiments) of SCIANTIX coupled with the abovementioned FPCs is out of the scope of the present work and will be the object of a separate ongoing work of the authors.

2.1. Physics-based models

The current section presents rate theory models available in SCIANTIX to describe the evolution of inert gases (xenon, krypton, and helium) within the nuclear fuel, considering fundamental intra- and inter-granular processes. Specifically, the processes considered comprise intra-granular gas diffusion, bubble nucleation, growth by trapping and interactions of gas bubbles with high-energy fission fragments, which may give rise to re-solution events of xenon and krypton atoms, otherwise insoluble, from the bubbles back into the ceramic matrix. Afterwards, accumulation of gas atoms in grain-face bubble is considered, together with phenomena of bubble growth, interconnection, coalescence, and grain-face saturation. As a result, SCIANTIX calculates the fission gas release (FGR) and local gaseous swelling of the fuel, as an inherently coupled phenomenon. This description is applied both to stable fission gas isotopes (to evaluate FGR and gaseous fuel swelling), and to radioactive fission gas isotopes (to evaluate the radioactive release from the fuel). Additionally, IGB modelling is sided with the fuel microstructure evolution, following the average grain size increase and peculiar phenomena relevant for high-burnup structure (HBS) description.

2.2. Intra-granular gas behaviour

SCIANTIX considers the behaviour of inert fission gases (xenon and krypton) at the grain scale via physics-based models, by assuming uniform temperature T, fission rate F, and hydrostatic stress σ_h (units of measure are reported in the Nomenclature).

In particular, the code models *intra-granular* fission gas diffusion in a spherical fuel grain of radius a (i.e., Booth approach [82]). The system of equations considers the diffusion equation for the fission gas concentration in the fuel matrix, available as single gas-atoms c, the rate

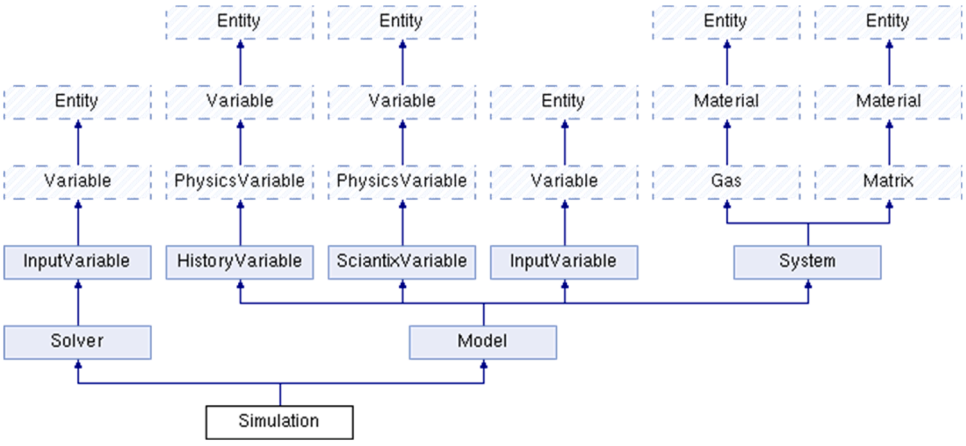

Fig. 2. Inheritance diagram (made with the Doxygen tool [73]) for the SCIANTIX simulation-object. The diagram illustrates the current internal SCIANTIX architecture and the hierarchical classification among defined objects.

equation for gas trapped within intra-granular bubbles m,[3] disregarding the diffusivity of intra-granular bubbles,[4] and the intra-granular bubble concentration N_{ig} [83]:

$$\begin{cases} \dfrac{\partial c}{\partial t} = D\dfrac{1}{r^2}\dfrac{\partial}{\partial r}r^2\dfrac{\partial c}{\partial r} + bm - gc + S \\ \dfrac{\partial m}{\partial t} = -bm + gc \\ \dfrac{\mathrm{d}N_{ig}}{\mathrm{d}t} = \nu - bN_{ig} \end{cases} \tag{1}$$

D is the single gas-atom diffusivity (Table 1), b is the re-solution rate (Table 2), g is the trapping rate[5] (Table 3), S is the source rate (equal to yF, y being the cumulative yield and F the fission rate density, respectively), r is the radial coordinate within the grain, and t is the time. The evolution of the intra-granular bubble concentration N_{ig} assumes that bubbles are formed at a nucleation rate ν (Table 4) and destroyed due to the irradiation induced re-solution with a rate b [22,84].

Table 1
Options available for intra-granular fission gas diffusivity D.

Option	Correlation	Reference
0	Trial constant value	–
1	$D\ (\mathrm{m^2 s^{-1}}) = 7.6 \times 10^{-10}\exp(-4.86 \times 10^{-19}/k_B T) + 5.64 \times 10^{-25}\sqrt{F}\exp(-1.91 \times 10^{-19}/k_B T) + 8 \times 10^{-40} F$	[85]
2	$D\ (\mathrm{m^2 s^{-1}}) = 5.0 \times 10^{-8}\exp(-40262/T)$	[86]

Table 2
Options available for intra-granular resolution rate b.

Option	Correlation	Reference
0	Trial constant value	–
1	(Irradiation-induced resolution rate) $b\ (\mathrm{s^{-1}}) = 2\pi\mu_{ff}(R_{ig} + R_{ff})^2 F$ $\mu_{ff} = 6.0 \times 10^{-6}$ m, fission fragment track length $R_{ff} = 1$ nm, fission fragment track radius	[85]
2	(Irradiation-induced resolution rate) $b\ (\mathrm{s^{-1}}) = 3.0 \times 10^{-23} F$	[87]
3	(Irradiation-induced and thermal resolution rate for helium behaviour) $b\ (\mathrm{s^{-1}}) = 2\pi\mu_{ff}(R_{ig,He} + R_{ff})^2 F + \gamma$ $\gamma\ (\mathrm{s^{-1}})$, thermal resolution rate (Eq. (8))	

Table 3
Options available for intra-granular trapping rate g.

Option	Correlation	Reference
0	Trial constant value	–
1	$g\ (\mathrm{s^{-1}}) = 4\pi D(R_{ig} + R_{sg})N_{ig}$ $\mu_{ff} = 6.0 \times 10^{-6}$ m, fission fragment track length R_{sg} (m) atom radius in the fuel lattice	[88]

Table 4
Options available for intra-granular bubble nucleation rate ν.

Option	Correlation	Reference
0	Trial constant value	–
1	$\nu\ (\mathrm{bub\ m^{-3} s^{-1}}) = 2\eta F$ $\eta = 25$ bubbles per fission fragment	[29,89,90]

From the numerical point of view, in Eq. (1), the concentrations c and m are calculated by exploiting the spectral diffusion algorithm [84,91,92] over the radial coordinate and the implicit Euler scheme in time. This approach makes SCIANTIX a mesh-free code and provides an *a priori* control on the numerical error depending on the time-step size and the number of modes selected for the spectral decomposition [91].

To calculate the intra-granular gaseous swelling, $(\Delta V/V)_{ig}$, the intra-granular bubble radius R_{ig} is first calculated by assuming that each

[3] In SCIANTIX it is possible to solve Eq. (1) for the gas concentrations c and m adopting the approach proposed by Speight [140], i.e., assuming the quasi-stationary hypothesis for m and following the evolution of the total intra-granular gas concentration $(c+m)$ [29,108,111]. This leads to the following equation: $\frac{\partial}{\partial t}(c+m) = \frac{b}{b+g}D\frac{1}{r^2}\frac{\partial}{\partial r}r^2\frac{\partial}{\partial r}(c+m) + yF$. Alternatively, it is possible to overcome the quasi- stationary approximation and solve Eq. (1) for the gas concentrations c and m with a direct matrix approach. The latter approach is necessary to simulate annealing experiments with nonzero intra-granular concentration.

[4] The intra-granular bubble mobility has been investigated in past works [13,31,141–145]. It has been considered to explain large fission gas releases at high temperatures (above 1600 °C) under annealing conditions and during transients, whereas it provides a negligible contribution to the fission gas release under normal reactor conditions [13]. Recent modelling analyses debated the role of the sole intra-granular bubble mobility on the observed fission gas release [141,144]. Therefore, because of the inherent uncertainty associated with this phenomenon, we disregard this effect for the time being.

[5] The default trapping rate adopted (Table 3) is the one from Ham [88], valid in the assumption that the trapping centre density is dilute enough.

bubble contains m/N_{ig} fission gas atoms.[6] Eventually, the intra-granular component of the gaseous swelling is calculated as:

$$\left(\frac{\Delta V}{V}\right)_{ig} = \frac{4}{3}\pi N_{ig} R_{ig}^3 \tag{2}$$

When fuel behaviour modelling implies the use of the physical fuel grain, average grain size evolution must be considered. Indeed, two mechanisms are considered as a consequence of the grain growth: (i) the intra-granular diffusion rate D/a^2 decreases, (ii) the grain-boundary sweeping can act as an additional contribution to the release of insoluble atoms at the grain boundary.

Given the importance of modelling grain growth for predicting FGR and gaseous fuel swelling, SCIANTIX includes laws of the following form, for the average grain size evolution:

$$\frac{\mathrm{d}D_{gr}}{\mathrm{d}t} = \frac{k^*}{D_{gr}^n} \tag{3}$$

where D_{gr} (m) is the average grain size and k^* ($m^2\ s^{-1}$) is the rate constant. The conversion between average grain size and spherical grain radius ($1.56D_{gr} = 2a$) is due to Mendelson [93]. The exponent n and the rate constant k^* are usually determined through fitting with experimental data. Semi-empirical laws of this type turn out to be easily applicable to codes that analyse single-grain behaviour of nuclear fuels and are compatible with the required short computation times. The models available in SCIANTIX are listed in Table 5.

Complementary to the grain growth, it is possible to consider the phenomenon of grain-boundary sweeping. This is crucial when considering the behaviour of intra-granular helium under annealing conditions [8,33,34]. Hence, the grain-boundary sweeping can be considered by modelling the swept volume fraction as in the TRANSURANUS code [21]. Ultimately, the fraction of intra-granular gas concentration c swept is $\mathrm{d}c/c = -\mathrm{d}V/V$, V being the swept volume due to grain growth.

2.3. Inter-granular gas behaviour

The *inter-granular* bubble evolution model currently available in SCIANTIX is the one proposed by Pastore et al. [7,96], extended to consider the micro-cracking of grain boundaries during temperature transients [9,97]. First, the fission gas arriving from the intra-granular diffusion is accumulated directly within bubbles. The rate equation for the inter-granular fission gas concentration q is:

Table 5
Options available for the grain growth.

Option	Correlation	Reference
0	The grain growth is not considered.	–
1	The grain growth is modelled according to the Ainscough et al. work. $\frac{\mathrm{d}D_{gr}}{\mathrm{d}t} = k\left(\frac{1}{D_{gr}} - \frac{f(\beta)}{D_{gr,lim}}\right)$	[94]
2	The grain growth is modelled according to the Van Uffelen et al. work. $\frac{\mathrm{d}D_{gr}}{\mathrm{d}t} = \frac{k}{4D_{gr}^3}$	[95]

[6] It is assumed that each xenon and krypton atom in UO_2 lattice occupies a Schottky trio volume ($\Omega = 4.09 \times 10^{-29}\ m^3\ at^{-1}$). Afterwards, the volume of an intra-granular bubble is given by $V_{ig} = m/N_{ig}$ and the radius $R_{ig} = \left(\frac{3}{4\pi}\frac{m}{N_{ig}}\Omega\right)^{\frac{1}{3}}$. This hypothesis is in line with the previous publication of SCIANTIX, where it is deeply justified [22].

$$\frac{\partial q}{\partial t} = -\left(\frac{3}{a}\frac{b}{b+g}D\frac{\partial(c+m)}{\partial r}\right)_a - R \tag{4}$$

The source term of Eq. (4) is the flux of single atoms arriving at the grain boundaries from within the fuel grain, evaluated from Eq. (1). Fission gas atoms that by diffusion reach the grain boundaries are immediately collected in inter-granular bubbles. It is assumed that gas atoms exist only in grain-boundary bubbles, and re-solution events from grain-boundary bubbles (back to the grain) are neglected. The thermal (or diffusional) release rate R is modelled by considering the evolution of bubbles on grain boundaries. The inter-granular bubble behaviour considers the following aspects. It is assumed that grain boundaries are populated with an initial number of bubbles N_{gf} (one-off nucleation). Grain-edge bubbles are not considered. Fission gas is continuously collected in grain-boundary bubbles, while bubble growth and coalescence occur. Bubble growth is related to the fact that grain-boundary bubbles are over-pressurized due to fission gases, hence in a non-equilibrium state, and tend to restore the equilibrium by absorption/emission of vacancies [98]. As bubbles grow, they interconnect and coalescence, resulting in a decreasing inter-granular bubble concentration N_{gf}, as their size increases. The net result of the inter-granular bubble growth, interconnection, and coalescence is the increase of the grain-face fractional coverage $F_{gf} = N_{gf}A_{gf}$ (/). When the fractional coverage reaches the saturation value $F_{gf} = F_{gf,sat} = 0.5$, it is assumed that the grain faces are vented, allowing for the (thermal or diffusional) release of gas from the grain boundaries.

To represent non-diffusional fission gas release during rapid temperature transients, known as burst fission gas release, SCIANTIX includes a semi-empiric description of the grain-face separation due to fuel micro-cracking. The model is based on the work of Barani et al. [9] and exploits typical quantities related to the mechanistic behaviour of grain-boundary bubbles. First, the model introduces the intactness of the grain faces f (/) and an empirical micro-cracking parameter, temperature-dependant $m_c(T)$. Then, when a temperature transient occurs ($\mathrm{d}T/\mathrm{d}t \neq 0$), the fractional coverage F_{gf} and saturation fractional coverage $F_{gf,sat}$ are scaled accordingly. The model is also able to represent the progressive healing of the grain-face as a purely burnup-dependant process. A complete description of model equations and performance can be found in Ref. [9].

Intrinsically tied to the mechanistic description of grain-boundary bubbles and FGR, the inter-granular component of the gaseous swelling is calculated as

$$\left(\frac{\Delta V}{V}\right)_{gf} = \frac{3}{a}\frac{4\pi}{3}N_{gf}R_{gf}^3 \tag{5}$$

where R_{gf} is the radius of inter-granular bubbles and $3/a$ is the surface-to-volume ratio of a spherical fuel grain.

2.4. High-burnup structure

The SCIANTIX code capabilities to describe fission gas behaviour in high burnup fuels have been progressively extended since the release of the code [22]. As previously stated, SCIANTIX operates at the grain scale, where the assumption of uniform temperature, fission rate, and hydrostatic stress are reasonable. This working hypothesis requires caution when SCIANTIX simulates the rim region of pellets in light water reactors, in which the self-shielding of thermal neutrons generates high gradients of fission rate.

As for behavioural models, several developments have been put into place targeting improved simulation capabilities of high burnup fuels. In synthesis:

- A fuel material representing the high burnup structure has been added to SCIANTIX, incorporating the properties of the restructured fuel (e.g., grain size and lattice parameter).

- The formation of the high burnup structure is based on a combination of an empirical threshold based on effective burnup [14,99,100] and Kolmogorov-Johnson-Mehl-Avrami (KJMA) model describing the fraction of fuel that undergoes restructuring [10].
- The high burnup structure porosity is based on an empirical model and predicted based on the local burnup [21,101].
- A physics-based model is considered for the evolution of the porosity distribution in terms of pore number density, average number of gas atoms per pore, and variance of the number of gas atoms per pore [11]. This model is derived from a Fökker-Planck approximation of the cluster dynamics master equations of pore-size evolution [83].
- The size of the high burnup structure pores is derived semi-empirically as a function of the porosity and the number density of pores, in line with state-of-the-art models available in similar codes [102].

With these developments, SCIANTIX simulates an abrupt transition from the standard UO_2 matrix (0 % HBS) to HBS matrix (100 % HBS). In the 100 % HBS matrix, SCIANTIX simulates fuel grains with a radius of 150 nm. Fission gas diffusion and release problems neglect intra-granular and inter-granular bubbles, whereas the HBS porosity is considered.

2.5. Helium behaviour

Given the importance of helium behaviour for fast reactor and storage conditions, mechanistic rate-theory models have been developed, implemented, and validated [8,103–105]. This section describes model and parameters currently available in the new SCIANTIX version to describe the helium behaviour, that follows essentially the work of Cognini et al. [8]. To provide satisfactory and applicable helium mechanistic modelling, the helium solubility in nuclear fuel must be considered, following Henry's Law [8,104,106,107]:

$$c_{lim} = k_H p \tag{6}$$

where k_H is the Henry's constant for the system He-UO_2 and c_{lim} is the solubility achieved at a pressure p. Intra-granular helium behaviour is formulated according to the generalization of the Speight's rate theory proposed by Van Uffelen et al. [33,108], disregarding the mobility of intra-granular bubbles [8]:

$$\begin{cases} \dfrac{\partial c_{\mathrm{He}}}{\partial t} = D_{\mathrm{He}} \dfrac{1}{r^2} \dfrac{\partial}{\partial r} r^2 \dfrac{\partial}{\partial r} c_{\mathrm{He}} - g c_{\mathrm{He}} + \gamma m_{\mathrm{He}} + yF \\ \dfrac{\partial m_{\mathrm{He}}}{\partial t} = g c_{\mathrm{He}} - \gamma m_{\mathrm{He}} \end{cases} \tag{7}$$

Eq. (7) share a similar structure to the fission gas diffusion problem of Eq. (1), including intra-granular diffusivity D_{He} (Table 6), trapping rate (Table 3), irradiation-induced and thermal re-solution of helium atoms from intra-granular bubbles (Table 2). Indeed, from the numerical point of view the problem is tackled with the spectral diffusion algorithm, already in place for Eq. (1). The suggested intra-granular helium diffusivities D_{He} are best-estimate correlations from the work of Luzzi et al. [103].

The thermal re-solution rate γ can be written as:

$$\gamma = 3 D_{\mathrm{He}} k_H k_B T Z \Big/ R_{\mathrm{ig,He}}^2 \tag{8}$$

Z being the compressibility factor (evaluated from the Van Brutzel et al. [59] equation of state). The adopted Henry's constant for helium in UO_2 is the best-estimate correlation for UO_2 single crystals selected after the review of Cognini et al. [104]:

$$k_H = 4.1 \times 10^{24} \exp(-7543.5 / T) \tag{9}$$

In the temperature range of 1073–1773 K, helium solubility within the UO_2 fuel grain is reasonably described by Eq. (9).

2.6. Radioactive fission gas behaviour

Accurate prediction of the radioactivity potentially released due to cladding failure is important, for example, to assess the radiological consequences of postulated accidental scenarios in nuclear reactors or to identify cladding failures during normal operation (e.g., due to fretting [109,110]). Therefore, it becomes important to evaluate the amount of radioactive gaseous and volatile fission products that accumulate in the free volume of the fuel rod, potentially available to be released into the primary circuit of a light water reactor. This section describes the mechanistic model available in the new version of SCIANTIX, to describe the behaviour of radioactive fission gases. The model, outlined in [91,111], was developed as a mechanistic alternative to the semi-empirical ANS-5.4–2010 approach [112], and has been tested in SCIANTIX, both in its standalone version and coupled with TRANSURANUS [53,111].

As proposed for stable fission gases (Sections 3.1 and 3.2) and helium (Section 3.4) behaviour, radioactive fission gas modelling includes the intra-granular and the inter-granular behaviour. The intra-granular gas behaviour starts from the time-dependant diffusion-decay equation within an ideal spherical grain. With the same assumptions used to formulate Eq. (1), the starting point for the intra-granular problem is the diffusion-decay equation for the gas concentration, available as single-atom (c), and the rate equation for gas within intra-granular bubbles (m),[7] disregarding the diffusivity of intra-granular bubbles:

$$\begin{cases} \dfrac{\partial c}{\partial t} = \alpha D \dfrac{1}{r^2} \dfrac{\partial}{\partial r} r^2 \dfrac{\partial c}{\partial r} + bm - gc - \lambda c + yF \\ \dfrac{\partial m}{\partial t} = -bm + gc - \lambda m \end{cases} \tag{10}$$

In Eq. (10), the combined effect of trapping-in (g) and irradiation-induced re-solution (b) from intra-granular bubbles is included along with the radioactive decay (λ is the decay rate of the radioactive isotope).

The intra-granular diffusivity is corrected through the precursor enhancement factor α (/), a corrective factor which takes into consideration the diffusivity increase that was observed for some radioactive gaseous and volatile fission product [113]. As reported in the ANS 5.4–2010 methodology [112] and based on the work of Friskney et al.

Table 6
Options available for helium intra-granular diffusivity ($m^2\ s^{-1}$).

Option	Correlation	Reference
0	$D_{\mathrm{He}}\ (\mathrm{m^2 s^{-1}}) = 0$	–
1	$D_{\mathrm{He}}\ (\mathrm{m^2 s^{-1}}) = 2 \times 10^{-10} \exp(-24{,}603.3 / T)$ Best-estimate correlation for samples with no or very limited lattice damage.	[103]
2	$D_{\mathrm{He}}\ (\mathrm{m^2 s^{-1}}) = 3.3 \times 10^{-10} \exp(-19{,}032.8 / T)$ Best-estimate correlation for samples with significant lattice damage.	[103]

[7] As mentioned earlier for the numerical solution of Eq. (1), In SCIANTIX it is possible to solve Eq. (10) adopting the quasi-stationary approach proposed by Speight [141], extended for radioactive isotopes. Contrary to what is reported in previous works [29,111], the quasi-stationary hypothesis for the concentration of gas trapped in bubbles m in Eq. (10), reading as $bm = gc$, leads to an effective diffusivity $D_{\mathrm{eff}} = \alpha \frac{b}{b+g} D$ for the total concentration of intragranular gas $c_{\mathrm{tot}} = c + m$. It is also possible to overcome this quasi-stationary approximation and solve Eq. (10) for the gas concentrations c and m with a direct matrix approach, in other words solving the system of two coupled equations. Both methods apply a spectral diffusion algorithm in space, over the spherical domain of the ideal fuel grain, while using the first order Euler scheme in time [84,91,92].

[114], for the first precursor $\alpha = \left(\left(1-\left(\frac{y_0}{x_0}\right)^3\right) \Big/ \left(1-\left(\frac{y_0}{x_0}\right)^2\right)\right)^2$. In this expression, $y_0 = \sqrt{D_p/\lambda_p}$ and $x_0 = \sqrt{D_d/\lambda_d}$, where λ_p and λ_d are the decay rates of the precursor (p) and daughter (d) isotope, respectively. Similarly, D_p and D_d are the intra-granular diffusivities of the precursor (p) and daughter (d) isotope, respectively. Values of α for radioactive gaseous and volatile fission products are available in literature, [111, 112]. We report values for two short-lived fission gases of interest: ^{133}Xe is characterised by $\alpha = 1.25$, and ^{85m}Kr by $\alpha = 1.31$.

As for the evolution of intra-granular and inter-granular bubbles, it is assumed that their behaviour is mainly driven by stable fission gases (i.e., stable xenon and krypton). In other words, the assumption exploits the fact that short-lived fission gases are negligible in mass with respect to stable fission gases, hence not relevant in determining the onset for diffusional release.[8] As a closure for Eq. (10), the concentration of radioactive fission gases in grain-boundary bubbles obeys to:

$$\frac{\partial q}{\partial t} = -\left(\frac{3}{a}\alpha\frac{b}{b+g}D\frac{\partial(c+m)}{\partial r}\right)_a - \lambda q - R \tag{11}$$

In Eq. (11), the release rate R (at m^{-3} s^{-1}) is computed with the same approach for Eq. (4).

3. Results

This section illustrates the results of SCIANTIX calculations, compared against the results of separate-effect irradiation experiments. Following the behavioural models described in Section 3, we consider the experimental data in terms of intra- and inter-granular gaseous swelling, high-burnup structure porosity, helium release and release of short-lived fission gas isotopes.

3.1. Intra-granular gas behaviour

In line with the first SCIANTIX validation [22], calculations of the intra-granular gaseous swelling are re-assessed against the separate-effect experimental results provided by Baker [90], and shown in Fig. 3. More precisely, irradiated fuel samples belonging to this database were analysed by means of transmission electron microscopy to measure concentration and radius of intra-granular bubbles. SCIANTIX simulations are set up with irradiation histories of 5500 h, at a constant fission rate ($F = 10^{19}$ fiss m^{-3} s^{-1}, resulting in a burnup of approximately 6.5 GWd tUO$_2^{-1}$), constant temperatures and null hydrostatic stress. Default fission gas behavioural models and parameters are used, i.e., Turnbull's diffusivity [85], heterogeneous nucleation [29, 89,115], heterogeneous re-solution rate [29], diffusional trapping [88]. Lastly, intra-granular calculations benefit from the use of the Ainscough et al. model for the fuel grain growth [94].

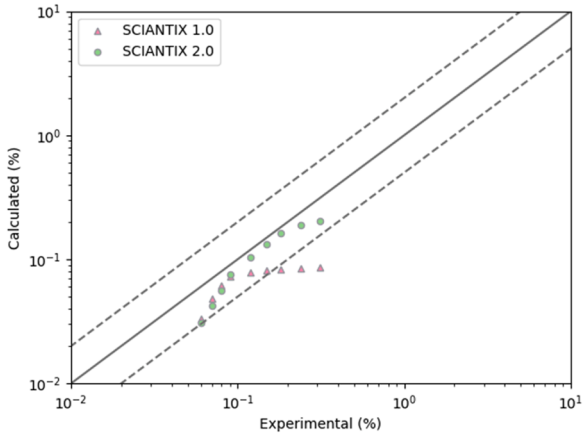

Fig. 3. Comparison of intra-granular gaseous swelling as calculated with SCIANTIX 1.0 (red triangles) and SCIANTIX 2.0 (green circles) against the experimental data by Baker [90]. Black dashed lines identify the double and half of the bisector of the graph (black solid line), respectively.

As a robust statistical figure merit, we choose the median of the absolute deviations (MAD) of the experimental data with respect to the code calculations. With respect to previous code calculations (red tr in Fig 3), MAD = 0.041), new SCIANTIX calculations better agree (MAD = 0.024) with the experimental data. This agreement is mainly due to swelling calculations above 0.1 %, induced by the grain growth process at high temperatures (> 1400 K), which allows more fission gas to be retained in larger grains and trapped due to diffusional trapping (Table 3).

3.2. Inter-granular gas behaviour

As for inter-granular gaseous swelling, and the application of SCIANTIX in fast transient conditions, the separate-effect validation database for the inter-granular model includes experimental cases from the database by White and co-workers [116]. The database consists in measurements performed on uranium dioxide AGR (Advanced Gas Reactor) samples of fuel rods irradiated up to burnup between 9 and 21 GWd/t$_{UO2}$ in the Halden reactor, followed by power ramp tests or power cycle histories. With respect to the original discussion about gaseous swelling calculations, i.e., the IGB during the transient as well as the simulation history set up, previous arguments hold [22]. The default fission gas behavioural models and parameters are used, i.e., Turnbull's diffusivity [85], heterogeneous nucleation [29,89,115], heterogeneous re-solution rate [29], diffusional trapping [88], Ainscough et al. model for the fuel grain growth [94], and Barani et al. grain-boundary micro-cracking [9]. Calculations of the new version of the code (green circles) and the experimental data are in good agreement (Fig. 4). With respect to the previous calculations (red triangles), the new calculations differ because of modifications concerning the more accurate implementation of the vacancy absorption/emission mechanisms at lenticular grain-boundary bubbles.

To conduct a thorough statistical analysis, required in this case given the number and dispersion of calculated and experimental points, we

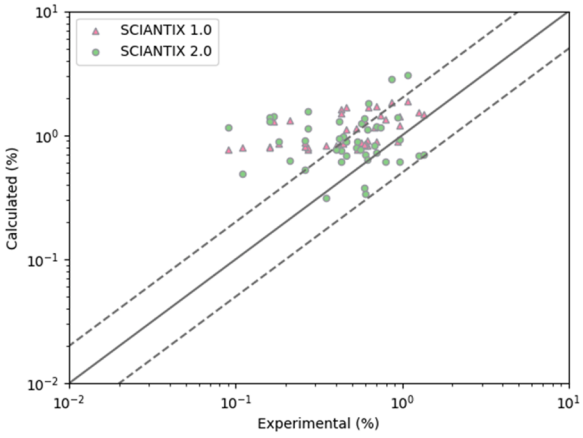

Fig. 4. Comparison of the experimental data for inter-granular gaseous swelling (from the database of White et al. [116]) against calculations obtained with SCIANTIX 1.0 (red triangles) and SCIANTIX 2.0 (green circles). Black dashed lines identify the double and half of the bisector of the graph (black solid line), respectively.

[8] This assumption is acceptable considering that the total mass inventory of fission products consists mainly of stable and long-lived fission products [145].

evaluate the MAD, the distribution of the experimental data as well as the distributions of SCIANTIX 1.0 and SCIANTIX 2.0 calculations (Fig. 5a), and the distribution of the error (predicted - measured) (Fig. 5b). Concerning the characteristics of the data distributions, it is noticeable how the new SCIANTIX version better represents the intergranular gaseous swelling distribution, hence the physical phenomenon, with respect to the calculations of the previous code version. Indeed, both first and third quartiles decrease, whereas the median keeps approximately the same value, providing a more centred distribution such as that obtained from the experimental data. Fig. 5b shows the distribution characteristics of the error between predicted and measured data. The MAD decreases from 0.52 (SCIANTIX 1.0) to 0.41 (SCIANTIX 2.0). Fig. 5b illustrates that SCIANTIX 1.0 provided a narrow overestimation of the experimental results, whereas SCIANTIX 2.0 includes regions below the bisector. Moreover, the two outliers are here superposed, suggesting a common reason for their overestimation.

3.3. High-burnup structure

Fig. 6 collects a set of representative results of the HBS model, compared with recent experimental data [117]. The semi-empiric nature of the model is clear in Fig. 6a, in which the porosity increase is assumed proportional to the local effective burnup up to 15 %. The nucleation of pores (Fig. 6b) is correlated with the KJMA-based rate of formation of the HBS (increase in pore number density from 50 to 100 GWd tHM^{-1}), followed by pore interconnection as the average pore radius increases (decrease in the pore number density above 100 GWd tHM^{-1}).

The current model also includes a physics-based description of the evolution with burnup of the HBS pore-size distribution (Fig. 6c). This feature is currently considering a one-dimensional phase space represented by the number of gas atoms per pore but can be extended towards a two-dimensional phase including the number of vacancies per pore. This extension is going to be critical in the future since it is linked with the capability of predicting a pressure distribution, which in turn allows physics-based modelling of fuel fragmentation. Lastly, from the pore number density and porosity calculations we obtain a semi-empirical description of the pore radius, depending on the local effective burnup (Fig. 6d).

As shown, the current version of SCIANTIX includes all the capabilities required for a semi-empirical description of high burnup structure formation and porosity evolution. These modelling capabilities are suitable for direct coupling within FPCs, in terms of numerical robustness, computational time, verification, and validation.

3.4. Helium behaviour

The physics-based model for helium behaviour has been applied to simulations of five separate-effect annealing experiments, illustrated in the work of Talip et al. [33]. Specifically, these experiments are characterized by a heating phase (about 30 min, 10–30 K min^{-1}), followed by a holding at the annealing temperature (about 1–3 h). In two of the five annealing histories (1320 K, 1400 K case a) there are two temperature plateaux with the second heating phase up to 2200–2300 K, while in three histories (1400 K case b, 1600 K, 1800 K), the temperature decreases after the plateau. These experiments constitute an independent separate-effect validation database for the SCIANTIX code when modelling helium behaviour, release, and release rate. Helium behavioural models and parameters are used, i.e., Luzzi et al. [104] diffusivity for samples with significant lattice damage diffusivity [85], diffusional trapping [88]. Van Uffelen et al. model for the fuel grain growth [95] including grain-boundary sweeping. Below, (Figs. 7-11) the performance of the new SCIANTIX version in terms of helium release and release during annealing conditions is illustrated.

3.5. Radioactive gas behaviour

The radioactive gas behaviour model has been re-assessed against the CONTACT 1 experiment [118,119], an irradiation experiment belonging to the IFPE open-access database.[9] The radioactive gas model adopts the default fission gas behavioural models and parameters, i.e., Turnbull's diffusivity [85], heterogeneous nucleation [29,89,115], heterogeneous re-solution rate [29], diffusional trapping [88], Ainscough et al. model for the fuel grain growth [94], and Barani et al. grain-boundary micro-cracking [9]. The simulation result is shown in Fig. 12. Similarly to Section 4.2 for the calculated intergranular gaseous swelling, the calculations of the new SCIANTIX version differs from the calculations of the version 1.0 because of modifications concerning the implementation of the vacancy absorption/emission mechanisms at lenticular grain-boundary bubbles. Considering the medians of the absolute deviations, SCIANTIX 2.0 calculations improve with respect to the previously published results [111], with lower medians of the absolute deviations of about 0.042 (^{133}Xe) and 0.0085 (^{85m}Kr) against previous values 0.071 (^{133}Xe) and 0.013 (^{85m}Kr).

4. Discussion and future work

The previous section showcased simulations of separate-effect experiments, complemented by statistical analyses, which indicated that the SCIANTIX code manages to reproduce the behaviour of stable, radioactive fission gas, and helium in UO_2 grains, both qualitatively and quantitatively. It is worth emphasizing that we employed default values for all model parameters (e.g., single-atom diffusivity, trapping rate, etc.) without any calibration. The capability of the code to reproduce the IGB in nuclear fuel is of paramount importance for the development, verification, and validation of behavioural models. Additionally, it plays a crucial role in the calculation of engineering quantities (e.g., local gaseous swelling and gas release) for use in the version of SCIANTIX coupled with FPCs.

However, limitations in the present version of SCIANTIX lead to discrepancies in the simulated results. When modelling the development of intra-granular gaseous swelling (Fig. 3), the overall underestimation of the calculated swelling is supposedly ascribable to the lack of a physics-based model in SCIANTIX, describing the irradiation-induced re-solution mechanism of fission gas atoms from grain-boundary bubbles to the grain [120]. Similarly, it contributes to the general overestimation of the calculated inter-granular gaseous swelling **(**Fig. 4**).** Moreover, the two outliers in Fig. 5 stem from two experiments (4064–1 and 4064–2) belonging to the database by White and co-workers [116]. These experiments exhibit peculiar conditions due to relatively high irradiation time and local fuel temperature [116,121]**)** which presumably induce substantial growth of grain-face bubbles that could be mitigated by the re-solution process.

To address these limitations, the development of a rate-theory physics-based model describing the irradiation-induced re-solution of fission gas atoms from grain-face bubbles is a future development of potential interest for the SCIANTIX code. Models already available in the open literature, as the one developed by Lösönen [120] includes parameters affected by large uncertainties. In this direction, atomistic and molecular dynamics studies on the re-solution of xenon gas bubbles may be crucial in accurately determining lower-length scale parameters, as

[9] The SCIANTIX input quantities required to perform the surrogate 0D simulation of the CONTACT 1 experiment (fuel temperature, fission rate density, and fuel hydrostatic stress) were derived by averaging radial quantities obtained from the TRANSURANUS simulation. Previous works [53,54,111] have shown that the use of lumped parameters (e.g., radial average of the fuel temperature and of the fuel hydrostatic stress) instead of radial profiles mainly influences the onset of thermal release, without influencing the asymptotic release-to-birth ratio of radioactive isotopes.

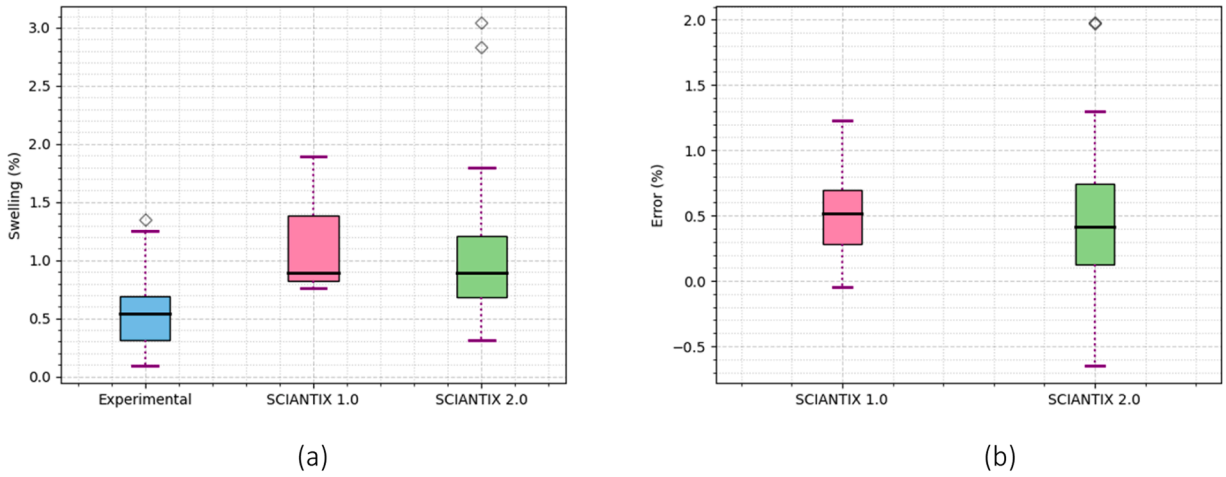

Fig. 5. (a) Distribution characteristics for the experimental data of inter-granular gaseous swelling from White et al. [116], SCIANTIX 1.0 [22] and SCIANTIX 2.0. (b) Distribution characteristics of the error (predicted – measured) for SCIANTIX 1.0 and SCIANTIX 2.0. White diamonds in boxplots identify outlier points.

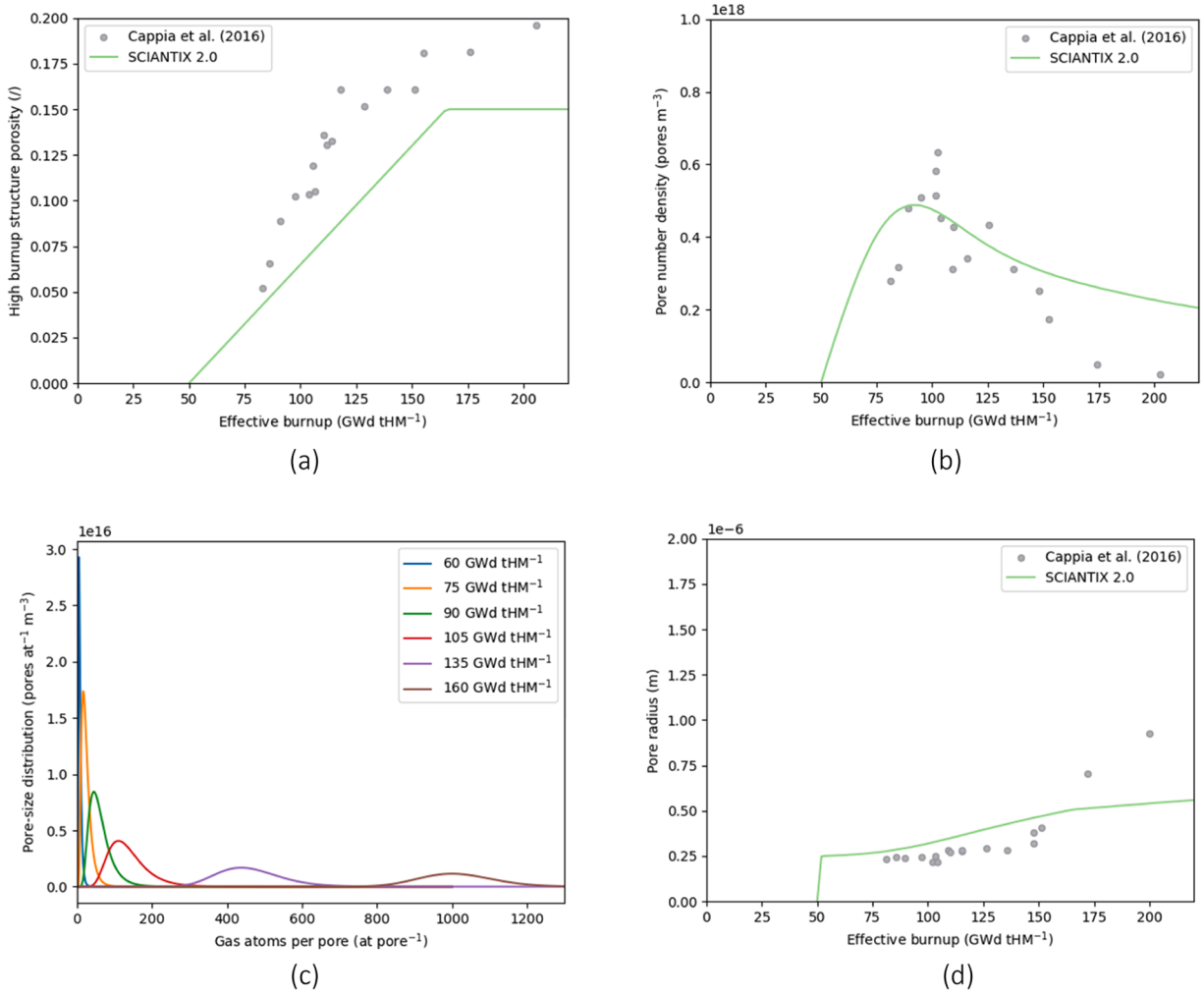

Fig. 6. Results of the behavioural model describing high-burnup structure in SCIANTIX. The model includes, (a) a semi-empirical description of the high-burnup structure porosity proportional to the local effective burnup, (b) a description of the pore number density based on Kolmogorov-Johnson-Mehl-Avrami high-burnup structure formation rate and pore interconnection, (c) a physics-based description of the evolution of the pore-size distribution, and (d) the calculation of the average pore radius. The data are extracted from [117].

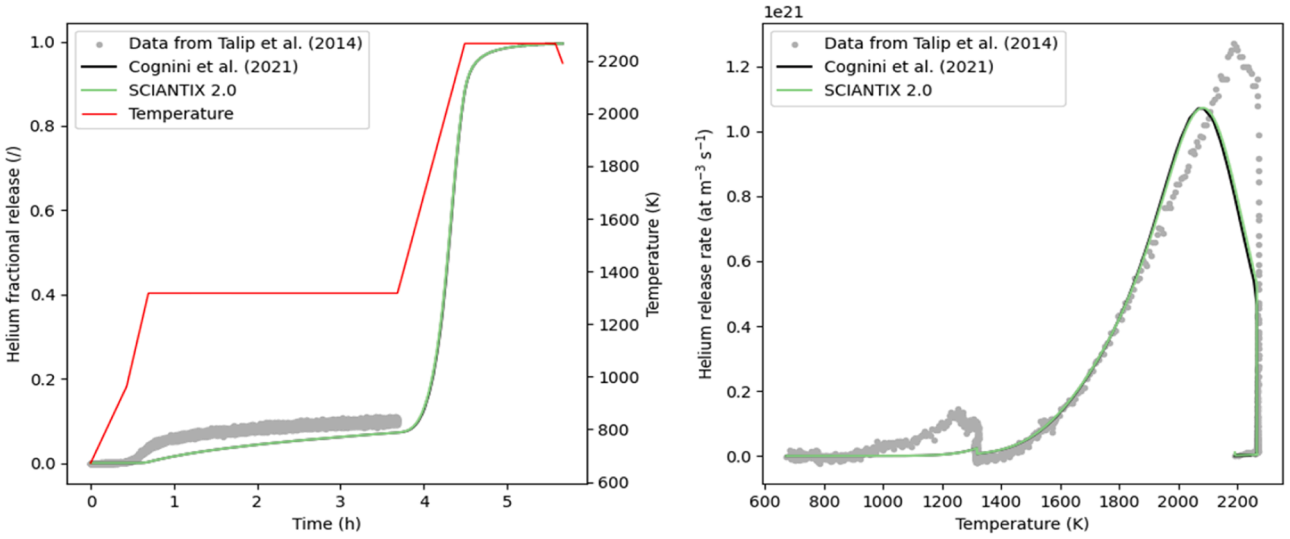

Fig. 7. Calculations of the new SCIANTIX version for helium fractional release (left) and release rate (right), against experimental data from Talip et al. work [33] and original calculations by Cognini et al. work [8], referred to the experimental test with the first temperature plateau at 1320 K.

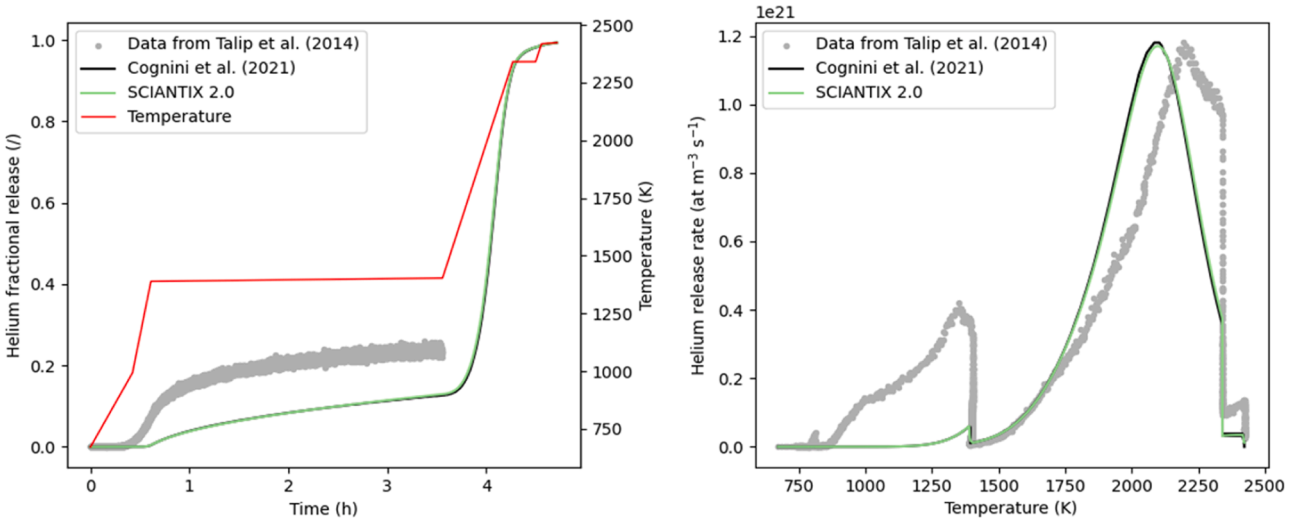

Fig. 8. Calculations of the new SCIANTIX version for helium fractional release (left) and release rate (right), against experimental data from Talip et al. work [33] and original calculations by Cognini et al. work [8], referred to the experimental test with the first temperature plateau at 1400 K (case a).

for the re-solution of intragranular xenon bubbles [122–124].

As for the helium behaviour, the SCIANTIX code preserves the modelling capabilities presented in the work of Cognini et al. [8] to describe the helium behaviour in nuclear fuel. Because Talip et al. annealing experiments were conducted on polycrystalline samples in vacuum conditions, the model predictions are driven by the sole intra-granular helium behaviour equation (Eq. (7)), neglecting the grain-boundary behaviour. Given that the model parameters (e.g., helium diffusivity) are independent of the validation database (e.g., not calibrated on experimental data), calculations provide a promising kinetic description of the helium released. Most of the observed differences are supposedly ascribable to the experimental uncertainty of key parameters that determine the helium thermal re-solution (e.g., the Henry's constant, for which few experimental data are available in the open literature [104]), and the lack of models for additional release mechanism, e.g., intra-granular bubble mobility, grain-boundary retention, pipe diffusion along grain boundaries, evaporation at higher temperatures (> 1700 K) with associated stoichiometry variations [125, 126].

Future development concerning behavioural models described in this work are going to include:

- A more mechanistic approach to describe the grain size evolution [127] and grain size distribution [128].
- A more mechanistic modelling of the grain-boundary microcracking due to sudden temperature variations, including a description of the pore-pressure distribution, in connection to the modelling of fuel fine fragmentation at high burnup.
- A physics-based model of the vacancy concentration in the HBS porosity, to overcome the empirical description currently in use in the code (Fig. 6a).
- The modelling of the dislocation network evolution [129], paired with considerations on the effect of the grain size in postponing HBS formation (e.g., in Cr-doped fuels [130]), overcoming the semi-empirical nature of the KJMA model.
- The implementation of a gradual transition from the UO_2–0 %HBS matrix and the UO_2–100 %HBS matrix, i.e., considering two fuel matrices simultaneously in the code.
- The implementation in the code of surrogate models trained on synthetic dataset, e.g., to capture the helium production rate in

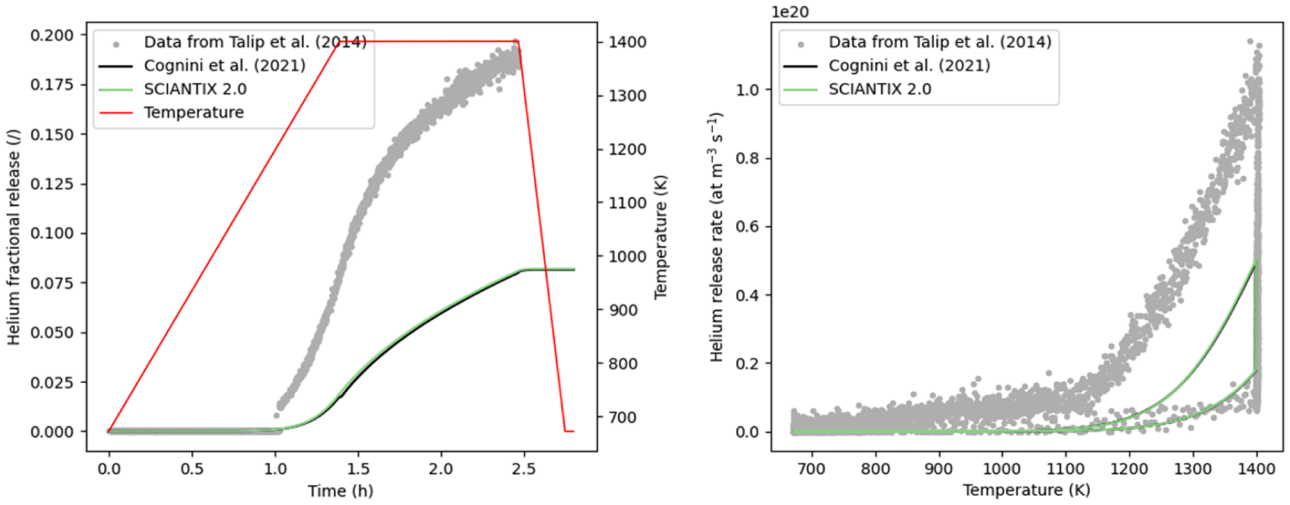

Fig. 9. Calculations of the new SCIANTIX version for helium fractional release (left) and release rate (right), against experimental data from Talip et al. work [33] and original calculations by Cognini et al. work [8], referred to the experimental test with the temperature plateau at 1400 K (case b).

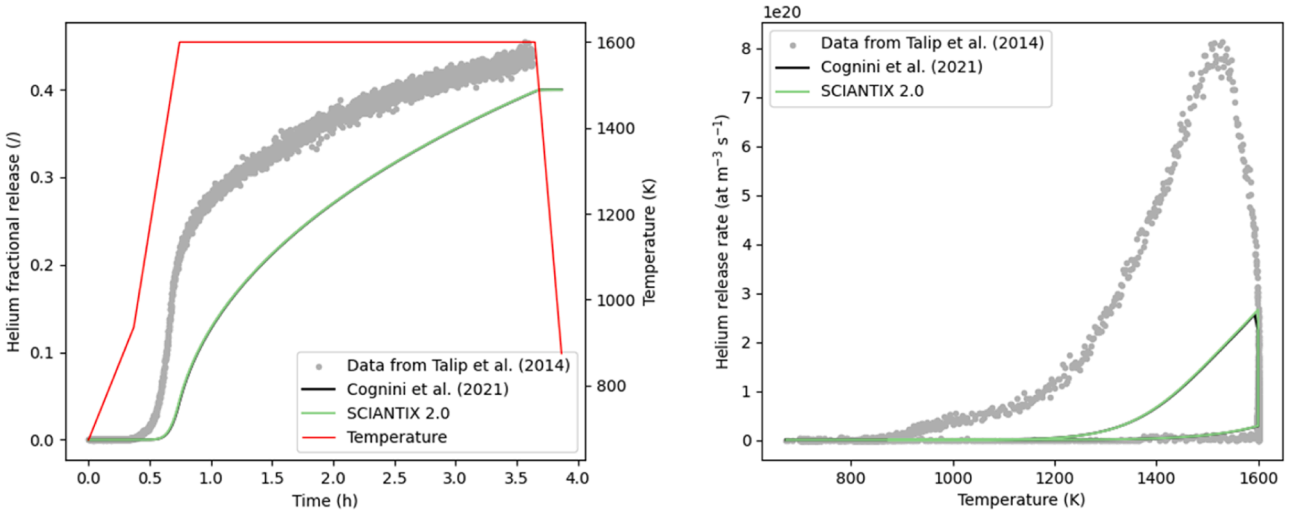

Fig. 10. Calculations of the new SCIANTIX version for helium fractional release (left) and release rate (right), against experimental data from Talip et al. work [33] and original calculations by Cognini et al. work [8], referred to the experimental test with the first temperature plateau at 1600 K.

uranium-plutonium mixed oxide fuels or americium-bearing fuels in fast reactor or storage conditions. The use of surrogate models equips SCIANTIX with fast-running correlations, inherently numerically stable, and with an accuracy level that satisfies the requirements of engineering tools such as fuel performance codes [79].

- New model parameters, as they become available either from experiments or lower-length scale calculations (e.g., re-solution rates [122], single-atom diffusivities [131], or equation-of-state parameters for helium-xenon mixture [132]), given the physics-based formulation of the models and the new SCIANTIX code structure that facilitates their implementation.

In addition, further developments of interest for the SCIANTIX modelling capabilities are:

- A comprehensive description of the fuel porosity, including the contributions from as-fabricated porosity, open porosity, and its evolution during irradiation [133,134].
- The description of standard UO_2 nuclear fuel doped with small amounts of metal oxides, such as Cr_2O_3, including its peculiarities such as the description of chromium solubility, and its impact on the fission gas behaviour [131,135].
- The description of chemically active radioactive volatile fission product behaviour (e.g., iodine, caesium and tellurium), including thermochemistry calculations, in conjunction with an underway modelling of fission gases in hyper-stoichiometric fuel [12,136,137].

These developments are currently being targeted in synergy with international partners and in the framework of international research projects [80,81,138,139]. Moreover, the validation of SCIANTIX coupled with integral FPCs, against integral irradiation experiments will be the object of a separate paper under preparation by the authors.

5. Conclusions

This work describes the status of SCIANTIX, a 0D, open-source code designed to model inert gas behaviour within nuclear fuel at the grain scale. The code is hosted online at [66], and it can be used both as a standalone module or coupled with integral codes, e.g., fuel performance codes. Since its first release, the code architecture has been revamped, and the numerical and modelling capabilities have been

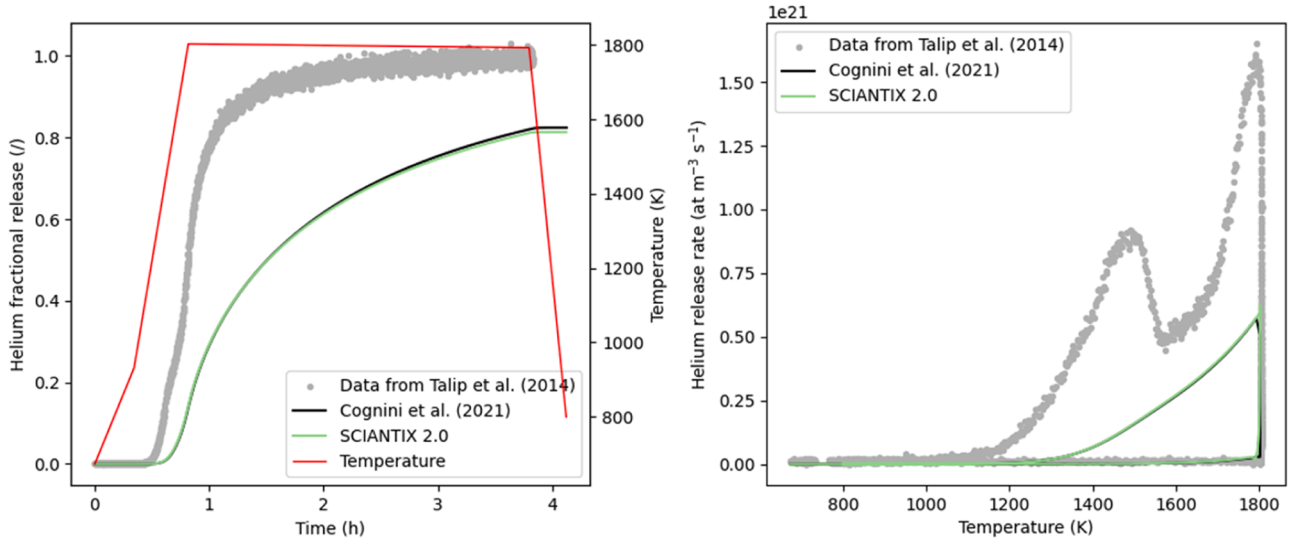

Fig. 11. Calculations of the new SCIANTIX version for helium fractional release (left) and release rate (right), against experimental data from Talip et al. work [33] and original calculations by Cognini et al. work [8], referred to the experimental test with the first temperature plateau at 1800 K.

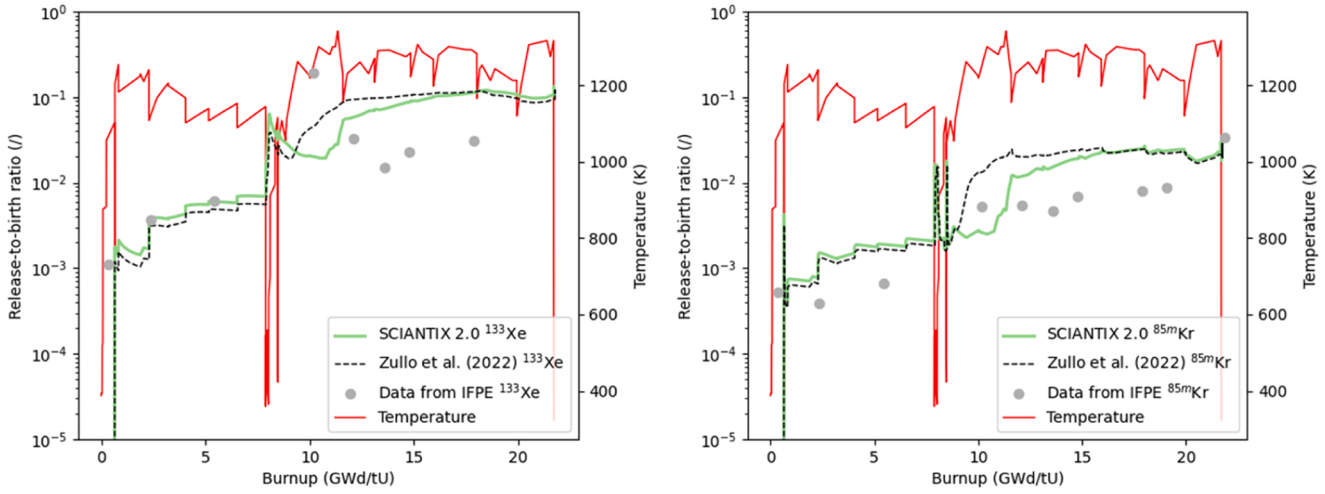

Fig. 12. Calculations of new SCIANTIX version for release-to-birth ratios of short-lived isotopes ^{133}Xe (left) and ^{85m}Kr (right), against data from CONTACT 1 [118, 119] experiments and original calculations by Zullo et al. [111].

extended. Physics-based models adopt kinetic rate-theory models to describe the evolution of inert gases (xenon, krypton and helium) within the nuclear fuel, considering fundamental intra- and inter-granular processes. This description is applied both to stable fission gas isotopes (to evaluate fission gas release and gaseous fuel swelling), and to radioactive fission gas isotopes (to evaluate the radioactive release from the fuel). Lastly, the inert gas behaviour modelling is sided with the fuel microstructure evolution, following evolution of the average grain size and peculiar phenomena relevant for high-burnup structure description. Physics-based models are presented together with the corresponding separate-effect validation.

Given the open-source nature of SCIANTIX, international standardised qualification and quality assurance guideline are being considered and integrated directly in the source code, e.g., concerning the code documentation via automated software documentation systems. In addition, the online code repository includes non-regression testing tools and continuous integration services that are going to be further extended and developed, to improve the process of testing new code versions and branches. The online repository also hosts the verification of the SCIANTIX numerical solvers, which facilitates separate developments on the numerical and physical aspects of the code.

CRediT authorship contribution statement

G. Zullo: Software, Investigation, Validation, Data curation, Visualization, Writing – original draft, Writing – review & editing. **D. Pizzocri:** Software, Supervision, Methodology, Validation, Visualization, Writing – review & editing. **L. Luzzi:** Resources, Supervision, Funding acquisition, Project administration, Visualization, Writing – review & editing.

Declaration of Competing Interest

The authors declare that they have no known competing financial interests or personal relationships that could have appeared to influence the work reported in this paper.

Data availability

Data will be made available on request.

Acknowledgements

The authors are grateful to A. Magni, S. Altieri, M. Bonacina, A. G. Carloni, A. Cechet, L. Cognini, M. Di Gennaro, A. Djonovic, R. Giorgi, M. G. Katsampiris, L. G. Mariano, B. Meleqi, G. Nicodemo, A. Pagani, G. Petrosillo, A. Piccini, E. Redaelli, M. Romano, G. Rota, F. Rotea, C. Valot, F. Verdolin, and S. Wang for their work on the code, and to T. Barani, M. Bertolus, M. Lainet, A. Schubert, A. Scolaro, F. Feria, L. E. Herranz, and P. Van Uffelen for their insight and support.

This project has received funding from the Euratom researchand training programme 2014-2018 under grant agreement n° 847656. This project has received funding from the Euratom research and training programme 2019–2020 through the PATRICIA Project under grant agreement n° 945077. This project has received funding from the Euratom research and training programme 2014–2018 through the INSPYRE project under grant agreement n° 754329. This project has received funding from the Euratom research and training programme 2021–2027 through the OperaHPC project under grant agreement n° 101061453. Views and opinions expressed in this paper reflect only the authors' view and the Commission is not responsible for any use that may be made of the information it contains.

References

[1] D.R. Olander, A.T. Motta. *Light Water Reactor Materials Volume I: Fundamentals*, American Nuclear Society, 2017.
[2] D.R. Olander, A.T. Motta. *Light Water Reactor Materials Volume II: Application*, American Nuclear Society, 2021.
[3] P. Van Uffelen, J. Hales, W. Li, G. Rossiter, R. Williamson, A review of fuel performance modelling, J. Nucl. Mater. 516 (2019) 373–412, https://doi.org/10.1016/j.jnucmat.2018.12.037.
[4] J. Rest, M.W.D. Cooper, J. Spino, J.A. Turnbull, P. Van Uffelen, C.T. Walker, Fission gas release from UO_2 nuclear fuel: a review, J. Nucl. Mater. 513 (2019) 310–345, https://doi.org/10.1016/j.jnucmat.2018.08.019.
[5] D. Pizzocri, L. Luzzi, T. Barani, L. Cognini, A. Magni, A. Schubert, P. Van Uffelen, T. Wiss, Review of available models and progress on the sub-models dealing with the intra- and intergranular inert gas behaviourINSPYRE Deliver. D612019.
[6] G. Pastore, T. Barani, D. Pizzocri, A. Magni, L. Luzzi, Modeling fission gas release and bubble evolution in UO_2 for engineering fuel rod analysis, in: Proceedings of Top Fuel, 2018.
[7] G. Pastore, L. Luzzi, V. Di Marcello, P. Van Uffelen, Physics-based modelling of fission gas swelling and release in UO_2 applied to integral fuel rod analysis, Nucl. Eng. Des. 256 (2013) 75–86, https://doi.org/10.1016/j.nucengdes.2012.12.002.
[8] L. Cognini, A. Cechet, T. Barani, D. Pizzocri, P. Van Uffelen, L. Luzzi, Towards a physics-based description of intra-granular helium behaviour in oxide fuel for application in fuel performance codes, Nucl. Eng. Technol. 53 (2) (2021) 562–571, https://doi.org/10.1016/j.net.2020.07.009.
[9] T. Barani, E. Bruschi, D. Pizzocri, G. Pastore, P. Van Uffelen, R.L. Williamson, L. Luzzi, Analysis of transient fission gas behaviour in oxide fuel using BISON and TRANSURANUS, J. Nucl. Mater. 486 (2017) 96–110, https://doi.org/10.1016/j.jnucmat.2016.10.051.
[10] T. Barani, D. Pizzocri, F. Cappia, L. Luzzi, G. Pastore, P. Van Uffelen, Modeling high burnup structure in oxide fuels for application to fuel performance codes. part I: high burnup structure formation, J. Nucl. Mater. 539 (2020), https://doi.org/10.1016/j.jnucmat.2020.152296.
[11] T. Barani, D. Pizzocri, F. Cappia, G. Pastore, L. Luzzi, P. Van Uffelen, Modeling high burnup structure in oxide fuels for application to fuel performance codes. Part II: porosity evolution, J. Nucl. Mater. 563 (2022), https://doi.org/10.1016/J.JNUCMAT.2022.153627.
[12] M.S. Veshchunov, V.D. Ozrin, V.E. Shestak, V.I. Tarasov, R. Dubourg, G. Nicaise, Development of the mechanistic code MFPR for modelling fission-product release from irradiated UO_2 fuel, Nucl. Eng. Des. 236 (2) (2006) 179–200, https://doi.org/10.1016/j.nucengdes.2005.08.006.
[13] P. Van Uffelen, G. Pastore, V. Di Marcello, L. Luzzi, Multiscale modelling for the fission gas behaviour in the TRANSURANUS Code, Nucl Eng Technol 43 (6) (2011) 477–488, https://doi.org/10.5516/NET.2011.43.6.477.
[14] G. Khvostov, Models for numerical simulation of burst FGR in fuel rods under the conditions of RIA, Nucl. Eng. Des. 328 (Mar. 2018) 36–57, https://doi.org/10.1016/J.NUCENGDES.2017.12.028.
[15] Y.H. Koo, B.H. Lee, D.S. Sohn, COSMOS: a computer code to analyze LWR UO_2 and MOX fuel up to high burnup, Ann Nucl Energy 26 (1) (1999) 47–67, https://doi.org/10.1016/S0306-4549(98)00033-4.
[16] G. Rossiter, Development of the enigma fuel performance code for whole core analysis and dry storage assessments, Nucl Eng Technol 43 (6) (2011) 489–498, https://doi.org/10.5516/NET.2011.43.6.489.
[17] J.D. Hales et al., "BISON Theory Manual The Equations behind Nuclear Fuel Analysis," Sep. 2016, 10.2172/1374503.
[18] J. Rest and S.A. Zawadzki, "FASTGRASS: a mechanistic model for the prediction of Xe, I, Cs, Te, Ba, and Sr release from nuclear fuel under normal and severe-accident conditions," Sep. 1992, 10.2172/7255051.
[19] G. Khvostov, K. Mikityuk, M.A. Zimmermann, A model for fission gas release and gaseous swelling of the uranium dioxide fuel coupled with the FALCON code, Nucl Eng Des 241 (8) (2011) 2983–3007, https://doi.org/10.1016/j.nucengdes.2011.06.020.
[20] L. Noirot, MARGARET: a comprehensive code for the description of fission gas behavior, Nucl Eng Des 241 (6) (2011) 2099–2118, https://doi.org/10.1016/j.nucengdes.2011.03.044.
[21] K. Lassmann, A. Schubert, P. Van Uffelen, C. Gyori, and J. van de Laar, TRANSURANUS Handbook, Copyright © 1975-2014. Institute for Transuranium Elements, Karlsruhe, 2014.
[22] D. Pizzocri, T. Barani, L. Luzzi, SCIANTIX: a new open source multi-scale code for fission gas behaviour modelling designed for nuclear fuel performance codes, J Nucl Mater 532 (2020) 152042, https://doi.org/10.1016/j.jnucmat.2020.152042.
[23] G. Jomard, C. Struzik, A. Boulore, P. Mailhé, V. Auret, R. Largenton, CARACAS. An industrial model for the description of fission gas behavior in LWR-UO_2 fuel, in: Proceedings of the water reactor fuel performance meeting, top fuel, LWR fuel performance meeting (WRFPM 2014), 2014. Available: http://inis.iaea.org/Search/search.aspx?orig_q=RN, 47079961.
[24] C.B. Lee, Y.S. Yang, D.H. Kim, S.K. Kim, J.G. Bang, A new mechanistic and engineering fission gas release model for a uranium dioxide fuel, J Nucl Sci Technol 45 (1) (2008) 60–71, https://doi.org/10.1080/18811248.2008.9711415.
[25] D. Yun, J. Rest, G.L. Hofman, A.M. Yacout, An initial assessment of a mechanistic model, GRASS-SST, in U–Pu–Zr metallic alloy fuel fission-gas behavior simulations, J. Nucl. Mater. 435 (1–3) (2013) 153–163, https://doi.org/10.1016/J.JNUCMAT.2012.12.024.
[26] J. Rest, A generalized model for radiation-induced amorphization and crystallization of U_3Si and U_3Si_2 and recrystallization of UO_2,", J. Nucl. Mater. 240 (3) (Feb. 1997) 205–214, https://doi.org/10.1016/S0022-3115(96)00714-3.
[27] J. Rest, A model for the influence of microstructure, precipitate pinning and fission gas behavior on irradiation-induced recrystallization of nuclear fuels, J. Nucl. Mater. 326 (2–3) (Mar. 2004) 175–184, https://doi.org/10.1016/J.JNUCMAT.2004.01.009.
[28] M.R. Tonks, et al., Mechanistic materials modeling for nuclear fuel performance, Ann Nucl Energy 105 (Jul. 2017) 11–24, https://doi.org/10.1016/J.ANUCENE.2017.03.005.
[29] R.J. White, M.O. Tucker, A new fission-gas release model, J. Nucl. Mater. 118 (1) (1983) 1–38, https://doi.org/10.1016/0022-3115(83)90176-9.
[30] M.S. Veshchunov, V.I. Tarasov, Modelling of irradiated UO_2 fuel behaviour under transient conditions, J. Nucl. Mater. 437 (1–3) (Jun. 2013) 250–260, https://doi.org/10.1016/J.JNUCMAT.2013.02.011.
[31] J.H. Evans, Bubble diffusion to grain boundaries in UO_2 and metals during annealing: a new approach, J. Nucl. Mater. 210 (1–2) (1994) 21–29, https://doi.org/10.1016/0022-3115(94)90218-6.
[32] M.S. Veshchunov, V.E. Shestak, Modelling of fission gas release from irradiated UO_2 fuel under high-temperature annealing conditions, J. Nucl. Mater. 430 (1–3) (2012) 82–89, https://doi.org/10.1016/j.jnucmat.2012.06.048.
[33] Z. Talip, T. Wiss, V. di Marcello, A. Janssen, J.Y. Colle, P. van Uffelen, P. Raison, R.J.M. Konings, Thermal diffusion of helium in ^{238}Pu-doped UO_2, J. Nucl. Mater. 445 (1–3) (2014) 117–127, https://doi.org/10.1016/j.jnucmat.2013.10.066.
[34] Z. Talip, et al., Helium behaviour in stoichiometric and hyper-stoichiometric UO_2, J Eur Ceram Soc 34 (5) (May 2014) 1265–1277, https://doi.org/10.1016/J.JEURCERAMSOC.2013.11.032.
[35] M. Stan, Discovery and design of nuclear fuels, Mater. Today 12 (11) (Nov. 2009) 20–28, https://doi.org/10.1016/S1369-7021(09)70295-0.
[36] E.A. Kotomin, Y.A. Mastrikov, S.N. Rashkeev, P. Van Uffelen, Implementing first principles calculations of defect migration in a fuel performance code for UN simulations, J. Nucl. Mater. 393 (2) (Sep. 2009) 292–299, https://doi.org/10.1016/J.JNUCMAT.2009.06.016.
[37] M. Bertolus, M. Freyss, B. Dorado, G. Martin, K. Hoang, S. Maillard, R. Skorek, P. Garcia, C. Valot, A. Chartier, L. van Brutzel, P. Fossati, R.W. Grimes, D. C. Parfitt, C.L. Bishop, S.T. Murphy, M.J.D. Rushton, D. Staicu, E. Yakub, R. K. Behera, Linking atomic and mesoscopic scales for the modelling of the transport properties of uranium dioxide under irradiation, J. Nucl. Mater. 462 (2015) 475–495, https://doi.org/10.1016/J.JNUCMAT.2015.02.026.
[38] Y. Miao, K.A. Gamble, D. Andersson, B. Ye, Z.G. Mei, G. Hofman, A.M. Yacout, Gaseous swelling of U_3Si_2 during steady-state LWR operation: A rate theory investigation, Nucl Eng. Des. 322 (2017) 336–344, https://doi.org/10.1016/J.NUCENGDES.2017.07.008.
[39] T. Barani, et al., Multiscale modeling of fission gas behavior in U_3Si_2 under LWR conditions, J. Nucl. Mater. 522 (2019) 97–110, https://doi.org/10.1016/j.jnucmat.2019.04.037.
[40] X.M. Bai, M.R. Tonks, Y. Zhang, J.D. Hales, Multiscale modeling of thermal conductivity of high burnup structures in UO_2 fuels, J. Nucl. Mater. 470 (Mar. 2016) 208–215, https://doi.org/10.1016/J.JNUCMAT.2015.12.028.
[41] M.R. Tonks, X.Y. Liu, D. Andersson, D. Perez, A. Chernatynskiy, G. Pastore, C. R. Stanek, R. Williamson, Development of a multiscale thermal conductivity model for fission gas in UO_2, J. Nucl. Mater. 469 (2016) 89–98, https://doi.org/10.1016/J.JNUCMAT.2015.11.042.
[42] D.A. Andersson, P. Garcia, X.Y. Liu, G. Pastore, M. Tonks, P. Millett, B. Dorado, D. R. Gaston, D. Andrs, R.L. Williamson, R.C. Martineau, B.P. Uberuaga, C.R. Stanek, Atomistic modeling of intrinsic and radiation-enhanced fission gas (Xe) diffusion

in $UO_{2\pm x}$: Implications for nuclear fuel performance modeling, J. Nucl. Mater 451 (1–3) (2014) 225–242, https://doi.org/10.1016/j.jnucmat.2014.03.041.
[43] L. Noirot, MARGARET: an advanced mechanistic model of fission gas behavior in nuclear fuel, J Nucl Sci Technol 43 (9) (2006) 1149–1160, https://doi.org/10.1080/18811248.2006.9711207.
[44] K. Lassmann, TRANSURANUS: a fuel rod analysis code ready for use, Nucl Mater Fiss React (1992) 295–302, https://doi.org/10.1016/b978-0-444-89571-4.50046-3.
[45] H.S. Aybar, P. Ortego, A review of nuclear fuel performance codes, Progr Nucl Energy 46 (2) (2005) 127–141, https://doi.org/10.1016/j.pnucene.2005.01.004.
[46] K. Lassmann, The structure of fuel element codes, Nucl Eng. Des. 57 (1) (Apr. 1980) 17–39, https://doi.org/10.1016/0029-5493(80)90221-6.
[47] R.L. Williamson, et al., Multidimensional multiphysics simulation of nuclear fuel behavior, J. Nucl. Mater. 423 (1–3) (Apr. 2012) 149–163, https://doi.org/10.1016/j.jnucmat.2012.01.012.
[48] J. Sercombe and M. le Saux, "D and 3D modelling of PCMI during a RIA with ALCYONE v1.1 enhanced acident tolerant fuels for nuclear light water reactors view project," 2010, Available: https://www.researchgate.net/publication/268801125.
[49] M.E. Cunningham, C.E. Beyer, P.G. Medvedev, F.E. Panisko, and G.A. Berna, "FRAPTRAN: a computer code for the transient analysis of oxide fuel rods," NUREG/CR-6739, Volume 1, 2001.
[50] J.Y.R. Rashid, S.K. Yagnik, and R.O. Montgomery, "Light water reactor fuel performance modeling and multi-dimensional simulation," JOM 2011 63:8, vol. 63, no. 8, pp. 81–88, Aug. 2011, 10.1007/S11837-011-0144-9.
[51] A. Scolaro, P. Van Uffelen, A. Schubert, C. Fiorina, E. Brunetto, I. Clifford, A. Pautz, Towards coupling conventional with high-fidelity fuel behavior analysis tools, Prog. Nucl. Energy 152 (2022), 104357, https://doi.org/10.1016/J.PNUCENE.2022.104357.
[52] A. Scolaro, I. Clifford, C. Fiorina, A. Pautz, The OFFBEAT multi-dimensional fuel behavior solver, Nucl Eng. Des. 358 (2020), 110416, https://doi.org/10.1016/J.NUCENGDES.2019.110416.
[53] G. Zullo, D. Pizzocri, A. Magni, P. Van Uffelen, A. Schubert, L. Luzzi, Towards grain-scale modelling of the release of radioactive fission gas from oxide fuel. Part II: coupling SCIANTIX with TRANSURANUS, Nucl. Eng. Technol. 54 (12) (Dec. 2022) 4460–4473, https://doi.org/10.1016/J.NET.2022.07.018.
[54] G. Zullo et al., "Final report on rod cladding failure during SGTR," pp. 1–65, 2023. Available: https://re.public.polimi.it/handle/11311/1233279.
[55] G. Zullo, et al., Towards simulations of fuel rod behaviour during severe accidents by coupling TRANSURANUS with SCIANTIX and MFPR-F, Ann Nucl Energy 190 (Sep. 2023), 109891, https://doi.org/10.1016/J.ANUCENE.2023.109891.
[56] D. Pizzocri, T. Barani, L. Luzzi, Coupling of TRANSURANUS with the SCIANTIX fission gas behaviour module, in: International Workshop "Towards Nuclear Fuel Modelling in the Various Reactor Types across, Europe (2019).
[57] T.R. Pavlov, F. Kremer, R. Dubourg, A. Schubert, P. Van Uffelen, Towards a more detailed mesoscale fission product analysis in fuel performance codes: a coupling of the TRANSURANUS and MFPR-F Codes, TopFuel (2018).
[58] L.Q. Chen, "Phase-field models for microstructure evolution vol. 32, pp. 113–140, Nov. 2003, 10.1146/annurev.matsci.32.112001.132041.
[59] L. Van Brutzel, A. Chartier, A new equation of state for helium nanobubbles embedded in UO_2 matrix calculated via molecular dynamics simulations, J. Nucl. Mater. 518 (May 2019) 431–439, https://doi.org/10.1016/J.JNUCMAT.2019.02.015.
[60] A. Magni, D. Pizzocri, L. Luzzi, M. Lainet, B. Michel, Application of the SCIANTIX fission gas behaviour module to the integral pin performance in sodium fast reactor irradiation conditions, Nucl. Eng. Technol. (2022), https://doi.org/10.1016/J.NET.2022.02.003.
[61] PTAN Qualification of scientific computing tools used in the nuclear safety case - 1st barrier - PTAN RC 20 001 Ind A. 2019.
[62] "IAEA Safety Standards for protecting people and the environment Specific Safety Guide Deterministic Safety Analysis for Nuclear Power Plants", 2023. Available: www.iaea.org/books.
[63] C. Herer, ASN/IRSN guide 28: qualification of scientific computing tools used in the nuclear safety case –1st barrier, Nucl Eng. Des. 405 (Apr. 2023), 112221, https://doi.org/10.1016/J.NUCENGDES.2023.112221.
[64] A. de surete nucleaire- ASN, I. de radioprotection et de surete nucleaire- IRSN, and IRSN, "Qualification of scientific computing tools used in the nuclear safety case - 1. barrier. Guide No. 28, Version of 25/07/2017." Jul. 25, 2017. Available: http://inis.iaea.org/Search/search.aspx?orig_q=RN:51079221.
[65] Deterministic Safety Analysis for Nuclear Power Plants, no. SSG-2. in Specific Safety Guides, Vienna: Int. Atom. Energy Age. (2010). Available: https://www.iaea.org/publications/8233/deterministic-safety-analysis-for-nuclear-power-plants.
[66] https://github.com/sciantix/sciantix-official.
[67] "DOI /sciantix · Zenodo." https://zenodo.org/badge/latestdoi/564329414.
[68] M. Lainet, B. Michel, J.C. Dumas, M. Pelletier, I. Ramière, GERMINAL, a fuel performance code of the PLEIADES platform to simulate the in-pile behaviour of mixed oxide fuel pins for sodium-cooled fast reactors, J. Nucl. Mater. 516 (Apr. 2019) 30–53, https://doi.org/10.1016/j.jnucmat.2018.12.030.
[69] "FRAPCON-4.0: a computer code for the calculation of steady-state, thermal-mechanical behavior of oxide fuel rods for high burnup.," 2015.
[70] S. MacNamara, G. Strang, Operator Splitting, in: R. Glowinski, S. Osher, W. Yin (Eds.), Splitting Methods in Communication, Imaging, Science, and Engineering. Scientific Computation, Springer, Cham, 2016. https://doi.org/10.1007/978-3-319-41589-5_3.
[71] W.L. Oberkampf, T.G. Trucano, Verification and validation in computational fluid dynamics, Prog. Aerosp. Sci. 38 (3) (2002) 209–272, https://doi.org/10.1016/S0376-0421(02)00005-2.
[72] W.L. Oberkampf, T.G. Trucano, C. Hirsch, Verification, validation, and predictive capability in computational engineering and physics, Appl. Mech. Rev. 57 (5) (2004) 345–384, https://doi.org/10.1115/1.1767847.
[73] D. Van Heesch, "Doxygen: source code documentation generator tool," 2008. http://www.doxygen.org.
[74] D. Pizzocri, T. Barani, L. Luzzi, Coupling of TRANSURANUS with the SCIANTIX fission gas behaviour module. International Workshop " Towards Nuclear Fuel Modelling in the Various Reactor Types Across Europe, 2019.
[75] M. Lainet, B. Michel, J.C. Dumas, M. Pelletier, I. Ramière, GERMINAL, a fuel performance code of the PLEIADES platform to simulate the in-pile behaviour of mixed oxide fuel pins for sodium-cooled fast reactors, J. Nucl. Mater. 516 (2019) 30–53, https://doi.org/10.1016/j.jnucmat.2018.12.030.
[76] "INSPYRE" http://www.eera-jpnm.eu/inspyre/.
[77] "PATRICIA." https://patricia-h2020.eu/.
[78] A. Magni, T. Barani, F. Belloni, B. Boer, E. Guizzardi, D. Pizzocri, A. Schubert, P. Van Uffelen, L. Luzzi, Extension and application of the TRANSURANUS code to the normal operating conditions of the MYRRHA reactor, Nucl. Eng. Des 386 (2022) 111581, https://doi.org/10.1016/J.NUCENGDES.2021.111581.
[79] D. Pizzocri, M.G. Katsampiris, L. Luzzi, A. Magni, G. Zullo, A surrogate model for the helium production rate in fast reactor MOX fuels, Nucl. Eng. Technol. 55 (8) (Aug. 2023) 3071–3079, https://doi.org/10.1016/J.NET.2023.04.044.
[80] https://r2ca-h2020.eu/.
[81] "OperaHPC." https://www.operahpc.eu/.
[82] A.H. Booth, *A method of calculating fission gas diffusion from UO_2 fuel and its application to the X-2-f loop test*. https://www.osti.gov/biblio/4331839.
[83] D. Pizzocri, et al., A model describing intra-granular fission gas behaviour in oxide fuel for advanced engineering tools, J. Nucl. Mater. 502 (2018) 323–330, https://doi.org/10.1016/j.jnucmat.2018.02.024.
[84] G. Pastore, D. Pizzocri, C. Rabiti, T. Barani, P. CVan Uffelen, L. Luzzi, An effective numerical algorithm for intra-granular fission gas release during non-equilibrium trapping and resolution, J. Nucl. Mater. 509 (2018) 687–699, https://doi.org/10.1016/j.jnucmat.2018.07.030.
[85] Turnbull, J. A., White, R. J., & Wise, C. (1989). The diffusion coefficient for fission gas atoms in uranium dioxide. In *(IWGFPT–32). International Atomic Energy Agency (IAEA)*. https://inis.iaea.org/search/search.aspx?orig_q=RN:21003206.
[86] H.J. Matzke, Gas release mechanisms in UO_2 —A critical review, Radiat Eff 53 (3–4) (1980) 219–242, https://doi.org/10.1080/00337578008207118.
[87] P. Lösönen, Modelling intragranular fission gas release in irradiation of sintered LWR UO_2 fuel, J. Nucl. Mater. 304 (1) (2002) 29–49, https://doi.org/10.1016/S0022-3115(02)00856-5.
[88] F.S. Ham, Theory of diffusion-limited precipitation, J Phys Chem Solids 6 (4) (1958) 335–351, https://doi.org/10.1016/0022-3697(58)90053-2.
[89] D.R. Olander, D. Wongsawaeng, *Re*-solution of fission gas - A review: part I. Intragranular bubbles, J. Nucl. Mater. 354 (1–3) (2006) 94–109, https://doi.org/10.1016/j.jnucmat.2006.03.010.
[90] C. Baker, The fission gas bubbles distribution in uranium dioxide from high temperature irradiated SGHWR fuel pins, J. Nucl. Mater. 66 (1977) 283–291.
[91] G. Zullo, D. Pizzocri, L. Luzzi, On the use of spectral algorithms for the prediction of short-lived volatile fission product release: methodology for bounding numerical error, Nucl. Eng. Technol. 54 (4) (2022) 1195–1205, https://doi.org/10.1016/J.NET.2021.10.028.
[92] D. Pizzocri, C. Rabiti, L. Luzzi, T. Barani, P. Van Uffelen, G. Pastore, PolyPole-1: an accurate numerical algorithm for intra-granular fission gas release, J. Nucl. Mater. 478 (2016) 333–342, https://doi.org/10.1016/j.jnucmat.2016.06.028.
[93] M.I. Mendelson, Average Grain Size in Polycrystalline Ceramics, J Am Ceram Soc 52 (8) (Aug. 1969) 443–446, https://doi.org/10.1111/J.1151-2916.1969.TB11975.X.
[94] J.B. Ainscough, B.W. Oldfield, J.O. Ware, Isothermal grain growth kinetics in sintered UO_2 pellets, J. Nucl. Mater. 49 (2) (1973) 117–128, https://doi.org/10.1016/0022-3115(73)90001-9.
[95] P. Van Uffelen, et al., An experimental study of grain growth in mixed oxide samples with various microstructures and plutonium concentrations, J. Nucl. Mater. 434 (1–3) (Mar. 2013) 287–290, https://doi.org/10.1016/j.jnucmat.2012.11.053.
[96] G. Pastore, et al., Uncertainty and sensitivity analysis of fission gas behavior in engineering-scale fuel modeling, J. Nucl. Mater. 456 (2015) 398–408, https://doi.org/10.1016/j.jnucmat.2014.09.077.
[97] G. Pastore, D. Pizzocri, J.D. Hales, S.R. Novascone, R.L. Williamson, B. W. Spencer, Modeling of transient fission gas behavior in oxide fuel and application to the BISON code, in: Proceedings of the Enlarged Halden Programme Group Meeting, Roros, Norway, 2014.
[98] M.V. Speigth, W. Beere, Vacancy Potential and Void Growth on Grain Boundaries, Acta Metals Soc (1975).
[99] L. Holt, A. Schubert, P. Van Uffelen, C.T. Walker, E. Fridman, T. Sonoda, Sensitivity study on Xe depletion in the high burn-up structure of UO 2, J. Nucl. Mater. 452 (1–3) (2014) 166–172, https://doi.org/10.1016/j.jnucmat.2014.05.009.
[100] D. Pizzocri, F. Cappia, L. Luzzi, G. Pastore, V.V. Rondinella, P. Van Uffelen, A semi-empirical model for the formation and depletion of the high burnup structure in UO_2, J. Nucl. Mater. 487 (2017) 23–29, https://doi.org/10.1016/j.jnucmat.2017.01.053.

[101] K. Lassmann, C.T. Walker, J. van de Laar, F. Lindström, Modelling the high burnup UO_2 structure in LWR fuel, J. Nucl. Mater. 226 (1–2) (1995) 1–8, https://doi.org/10.1016/0022-3115(95)00116-6.

[102] F. Kremer et al., "High Burn Up Structure formation and growth and fission product release modelling: new simulations in the mechanistic code MFPR-F".

[103] L. Luzzi, et al., Helium diffusivity in oxide nuclear fuel: critical data analysis and new correlations, Nucl Eng. Des. 330 (Apr. 2018) 265–271, https://doi.org/10.1016/J.NUCENGDES.2018.01.044.

[104] L. Cognini, et al., Helium solubility in oxide nuclear fuel: derivation of new correlations for Henry's constant, Nucl Eng. Des. 340 (Dec. 2018) 240–244, https://doi.org/10.1016/J.NUCENGDES.2018.09.024.

[105] R. Giorgi, et al., Physics-based modelling and validation of inter-granular helium behaviour in SCIANTIX, Nucl. Eng. Technol. 54 (7) (Jul. 2022) 2367–2375, https://doi.org/10.1016/J.NET.2022.01.012.

[106] F. Rufeh, D.R. Olander, and T.H. Pigford, "The Solubility of helium in uranium dioxide," *https://doi.org/10.13182/NSE65-A21069*, vol. 23, no. 4, pp. 335–338, Dec. 2017, 10.13182/NSE65-A21069.

[107] K. Nakajima, H. Serizawa, N. Shirasu, Y. Haga, Y. Arai, The solubility and diffusion coefficient of helium in uranium dioxide, J. Nucl. Mater. 419 (1–3) (Dec. 2011) 272–280, https://doi.org/10.1016/J.JNUCMAT.2011.08.045.

[108] M.V. Speight, A Calculation on the Migration of Fission Gas in Material Exhibiting Precipitation and *Re*-solution of Gas Atoms Under Irradiation, Nucl Sci Eng 37 (2) (1969) 180–185, https://doi.org/10.13182/nse69-a20676.

[109] K.T. Kim, The study on grid-to-rod fretting wear models for PWR fuel, Nucl Eng. Des. 239 (12) (Dec. 2009) 2820–2824, https://doi.org/10.1016/J.NUCENGDES.2009.08.018.

[110] S. Lazarevic, R.Y. Lu, C. Favede, G. Plint, P.J. Blau, J. Qu, Investigating grid-to-rod fretting wear of nuclear fuel claddings using a unique autoclave fretting rig, Wear 412–413 (Oct. 2018) 30–37, https://doi.org/10.1016/J.WEAR.2018.06.011.

[111] G. Zullo, D. Pizzocri, A. Magni, P. Van Uffelen, A. Schubert, L. Luzzi, Towards grain-scale modelling of the release of radioactive fission gas from oxide fuel . Part I: SCIANTIX, Nucl. Eng. Technol. (2022), https://doi.org/10.1016/J.NET.2022.02.011.

[112] Beyer, Carl E, and Turnbull, Andrew J. *Background and Derivation of ANS-5.4 Standard Fission Product Release Model*. United States: N. p., 2010. 10.2172/1033086.

[113] P.E. Brown, R.L. Faircloth, Metal fission product behaviour in high temperature reactors - UO_2 coated particle fuel, J. Nucl. Mater. 59 (1) (1976) 29–41, https://doi.org/10.1016/0022-3115(76)90005-2.

[114] C.A. Friskney, M.V. Speight, A calculation on the in-pile diffusional release of fission products forming a general decay chain, J. Nucl. Mater. 62 (1976) 89–94.

[115] J.A. Turnbull, The distribution of intragranular fission gas bubbles in UO_2 during irradiation, J. Nucl. Mater. 38 (2) (1971) 203–212, https://doi.org/10.1016/0022-3115(71)90044-4.

[116] R. White and J.A. Turnbull, "IFPE/CAGR-UOX-SWELL, Fuel swelling Data Obtained from the AGR/Halden Ramp Test Programme." Jun. 06, 2006. Available: https://inis.iaea.org/search/search.aspx?orig_q=RN:40064987.

[117] F. Cappia, et al., Critical assessment of the pore size distribution in the rim region of high burnup UO_2 fuels, J. Nucl. Mater. 480 (Nov. 2016) 138–149, https://doi.org/10.1016/J.JNUCMAT.2016.08.010.

[118] Bruet, M., Pointud, M. L., Dodelier, J., & Melin, P. H. (1980). Contact 1 and 2 experiments: behaviour of PWR fuel rod up to 15000 $MWd.tu^{-1}$. In *(IWGFPT–7). International Atomic Energy Agency (IAEA)*. https://inis.iaea.org/search/search.aspx?orig_q=RN:12622604.

[119] Charles, M., Abassin, J. J., Bruet, M., Baron, D., & Melin, P. (1983). Utilization of "'CONTACT"' experiments to improve the fission gas release knowledge in PWR fuel rods. In *(IWGFPT–13). International Atomic Energy Agency (IAEA)*. https://inis.iaea.org/search/search.aspx?orig_q=RN:17007025.

[120] P. Lösönen, On the effect of irradiation-induced resolution in modelling fission gas release in UO_2 LWR fuel, J. Nucl. Mater. 496 (Dec. 2017) 140–156, https://doi.org/10.1016/J.JNUCMAT.2017.09.015.

[121] R.J. White, The development of grain-face porosity in irradiated oxide fuel, J. Nucl. Mater. 325 (1) (2004) 61–77, https://doi.org/10.1016/j.jnucmat.2003.10.008.

[122] W. Setyawan, M.W.D. Cooper, K.J. Roche, R.J. Kurtz, B.P. Uberuaga, D. A. Andersson, B.D. Wirth, Atomistic model of xenon gas bubble re-solution rate due to thermal spike in uranium oxide, J Appl Phys 124 (7) (2018), 075107, https://doi.org/10.1063/1.5042770.

[123] K. Govers, C.L. Bishop, D.C. Parfitt, S.E. Lemehov, M. Verwerft, and R.W. Grimes, "Molecular dynamics study of Xe bubble re-solution in UO2," J Nucl Mater, vol. 420, no. 1–3, pp. 282–290, Jan. 2012, 10.1016/J.JNUCMAT.2011.10.010.

[124] M. Huang, D. Schwen, R.S. Averback, Molecular dynamic simulation of fission fragment induced thermal spikes in UO_2: sputtering and bubble re-solution, J. Nucl. Mater. 399 (2–3) (Apr. 2010) 175–180, https://doi.org/10.1016/J.JNUCMAT.2010.01.015.

[125] J.P. Hiernaut, T. Wiss, D. Papaioannou, R.J.M. Konings, V.V. Rondinella, Volatile fission product behaviour during thermal annealing of irradiated UO_2 fuel oxidised up to U_3O_8,", J. Nucl. Mater. 372 (2–3) (Jan. 2008) 215–225, https://doi.org/10.1016/J.JNUCMAT.2007.03.174.

[126] J.P. Hiernaut, T. Wiss, J.Y. Colle, H. Thiele, C.T. Walker, W. Goll, R.J.M. Konings, Fission product release and microstructure changes during laboratory annealing of a very high burn-up fuel specimen, J. Nucl. Mater. 377 (2) (2008) 313–324, https://doi.org/10.1016/J.JNUCMAT.2008.03.006.

[127] M.R. Tonks, P.C.A. Simon, J. Hirschhorn, Mechanistic grain growth model for fresh and irradiated UO_2 nuclear fuel, J. Nucl. Mater. 543 (Jan. 2021), 152576, https://doi.org/10.1016/J.JNUCMAT.2020.152576.

[128] P.C. Millett, Y. Zhang, M.R. Tonks, S.B. Biner, Consideration of grain size distribution in the diffusion of fission gas to grain boundaries, J. Nucl. Mater. 440 (1–3) (2013) 435–439, https://doi.org/10.1016/j.jnucmat.2013.05.065.

[129] Model for evolution of crystal defects in UO_2 under irradiation up to high burn-ups, J. Nucl. Mater. 384 (1) (Jan. 2009) 12–18, https://doi.org/10.1016/J.JNUCMAT.2008.09.024.

[130] J. Noirot, L. Desgranges, J. Lamontagne, Detailed characterisations of high burn-up structures in oxide fuels, J. Nucl. Mater. 372 (2–3) (Jan. 2008) 318–339, https://doi.org/10.1016/j.jnucmat.2007.04.037.

[131] M.W. Cooper, G. Pastore, Y. Che, C. Matthews, A. Forslund, C.R. Stanek, K. Shirvan, T. Tverberg, K.A. Gamble, B. Mays, D.A. Andersson, Fission gas diffusion and release for Cr2O3-doped UO2: From the atomic to the engineering scale, J. Nucl. Mater. 545 (2021) 152590, https://doi.org/10.1016/J.JNUCMAT.2020.152590.

[132] L. Van Brutzel, E. Castelier, Equation of state for helium-xenon gas mixture studied by molecular dynamics simulations, J. Nucl. Mater. 586 (Dec. 2023), 154654, https://doi.org/10.1016/J.JNUCMAT.2023.154654.

[133] V.I. Tarasov, M.S. Veshchunov, Modelling of as-fabricated porosity in UO_2 fuel by MFPR code, EPJ Nucl Sci Technol vol. 2 (2016) 19, https://doi.org/10.1051/EPJN/2016013.

[134] A. Claisse, P. Van Uffelen, Towards the inclusion of open fabrication porosity in a fission gas release model, J. Nucl. Mater. 466 (2015) 351–356, https://doi.org/10.1016/j.jnucmat.2015.08.022.

[135] A. R. Massih, L.O. Jernkvist, (2021). *2021:20 Effects of additives on UO_2 fuel behavior: expanded edition*. https://www.stralsakerhetsmyndigheten.se/publikationer/rapporter/sakerhet-vid-karnkraftverken/2021/202120/.

[136] A.R. Massih, *2018:25 UO_2 fuel oxidation and fission gas release*. https://www.stralsakerhetsmyndigheten.se/en/publications/reports/safety-at-nuclear-power-plants/2018/201825/.

[137] A. Germain, J. Sercombe, C. Riglet-Martial, C. Introïni, L. Noirot, Y. Pontillon, P. Maugis, Coupled modeling of irradiated fuel thermochemistry and gas diffusion during severe accidents, J. Nucl. Mater. 560 (2022) 153429, https://doi.org/10.1016/J.JNUCMAT.2021.153429.

[138] "Open-source Nuclear Codes for Reactor Analysis." https://nucleus.iaea.org/sites/oncore/SitePages/Home.aspx.

[139] Nuclear energy agency (NEA) - burst fission gas release (bFGR) benchmark of the expert group on reactor fuel performance (EGRFP). https://www.oecdnea.org/jcms/pl_70791/burst-fission-gas-release-fgr-benchmark-of-the-expert-group-on-reactor-fuel-performance-egrfp.

[140] L. Verma, L. Noirot, P. Maugis, Modelling intra-granular bubble movement and fission gas release during post-irradiation annealing of UO_2 using a meso-scale and spatialized approach, J. Nucl. Mater. 528 (2020), 151874, https://doi.org/10.1016/j.jnucmat.2019.151874.

[141] L. Verma, L. Noirot, P. Maugis, A new spatially resolved model for defects and fission gas bubbles interaction at the mesoscale, Nucl Instrum Methods Phys Res B 458 (2018) 151–158, https://doi.org/10.1016/j.nimb.2018.10.028.

[142] A. Moal, V. Georgenthum, O. Marchand, SCANAIR: a transient fuel performance code: part One: general modelling description, Nucl Eng. Des. 280 (Dec. 2014) 150–171, https://doi.org/10.1016/J.NUCENGDES.2014.03.055.

[143] M.E. Gulden, Migration of gas bubbles, J. Nucl. Mater. 23 (1967) 30–36.

[144] L. Noirot, L. Verma, P. Maugis, Oriented intra-granular bubble transport due to coupling of pinned bubble growth and dislocation climb, J. Nucl. Mater. 577 (Apr. 2023), 154311, https://doi.org/10.1016/J.JNUCMAT.2023.154311.

[145] B.R. Sehgal, Nuclear safety in light water reactors, Nucl Saf Light Water React (2012), https://doi.org/10.1016/C2010-0-67817-5.